Chap.4　Galactic Dark Matter

- Evidence for dark matter in the Milky Way
- Properties of a dark matter halo
  - Total mass, global shape, density profile, substructures
- Recent progress on small-scale issues
  - Missing satellites problem
  - Core/cusp problem
- Future prospects

1. Evidence of dark matter in the Milky Way

Jan Hendrik Oort

In 1932, Jan Oort suggested the presence of dark matter near the Sun ("missing mass") from the dynamical analysis of stellar motions

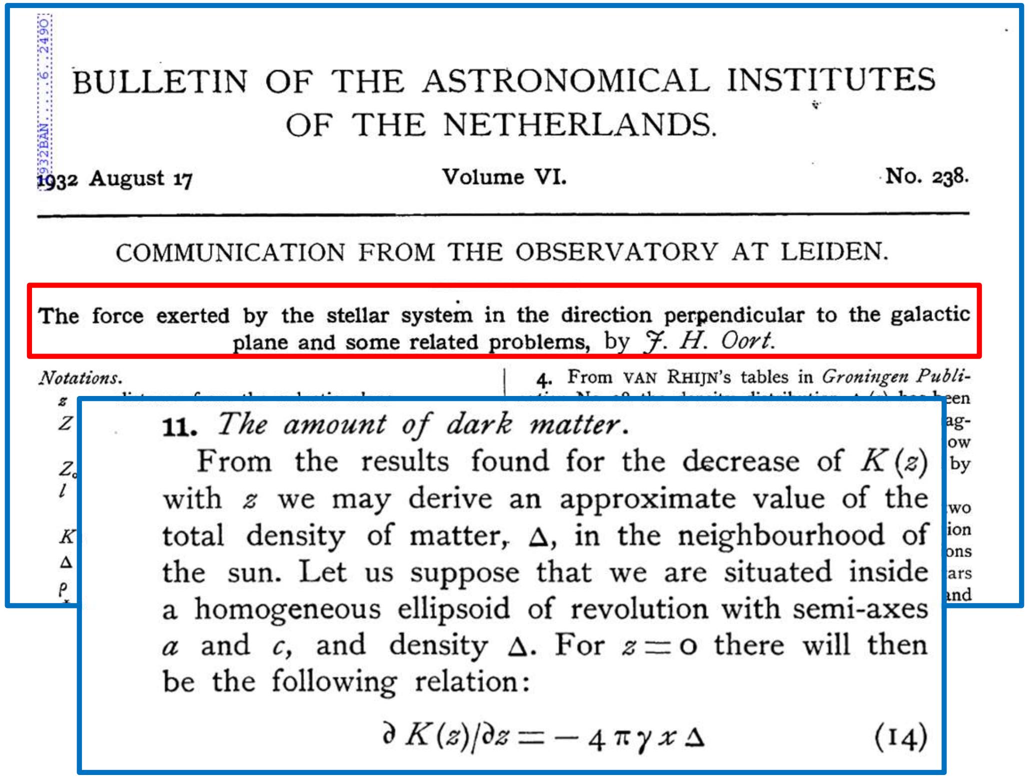

BULLETIN OF THE ASTRONOMICAL INSTITUTES OF THE NETHERLANDS.

1932 August 17 Volume VI. No. 238.

COMMUNICATION FROM THE OBSERVATORY AT LEIDEN.

The force exerted by the stellar system in the direction perpendicular to the galactic plane and some related problems, by *J. H. Oort.*

Notations.

4. From VAN RHIJN's tables in *Groningen Publi-*

11. *The amount of dark matter.*

From the results found for the decrease of $K(z)$ with z we may derive an approximate value of the total density of matter, Δ, in the neighbourhood of the sun. Let us suppose that we are situated inside a homogeneous ellipsoid of revolution with semi-axes a and c, and density Δ. For $z = 0$ there will then be the following relation:

$$\partial K(z)/\partial z = -4\pi\gamma x \Delta \qquad (14)$$

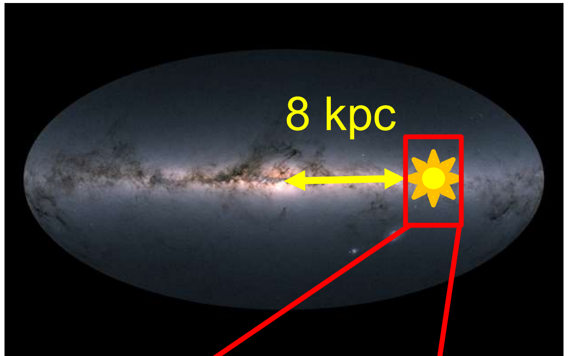

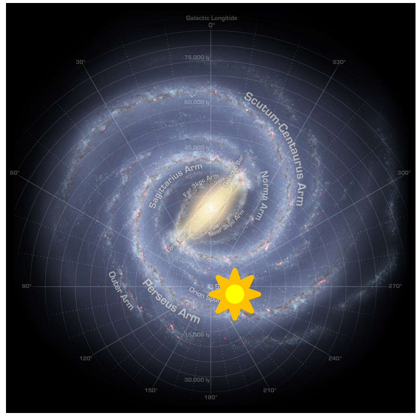

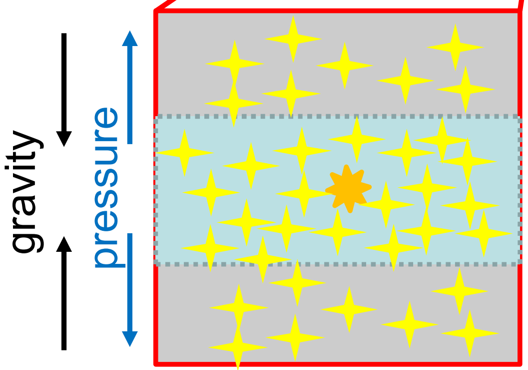

Pressure force due to the random motions of stars are in balance with gravity exerted from both visible and invisible matter

⇒visible mass is found to be insufficient

⇒missing mass, dark matter

Dark matter density near the Sun

Measured from the dynamical analysis of
the large number of nearby star sample

SDSS

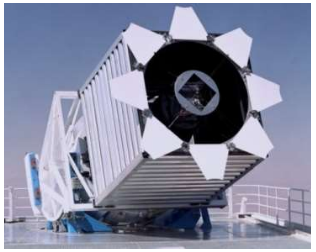

LAMOST

Gaia

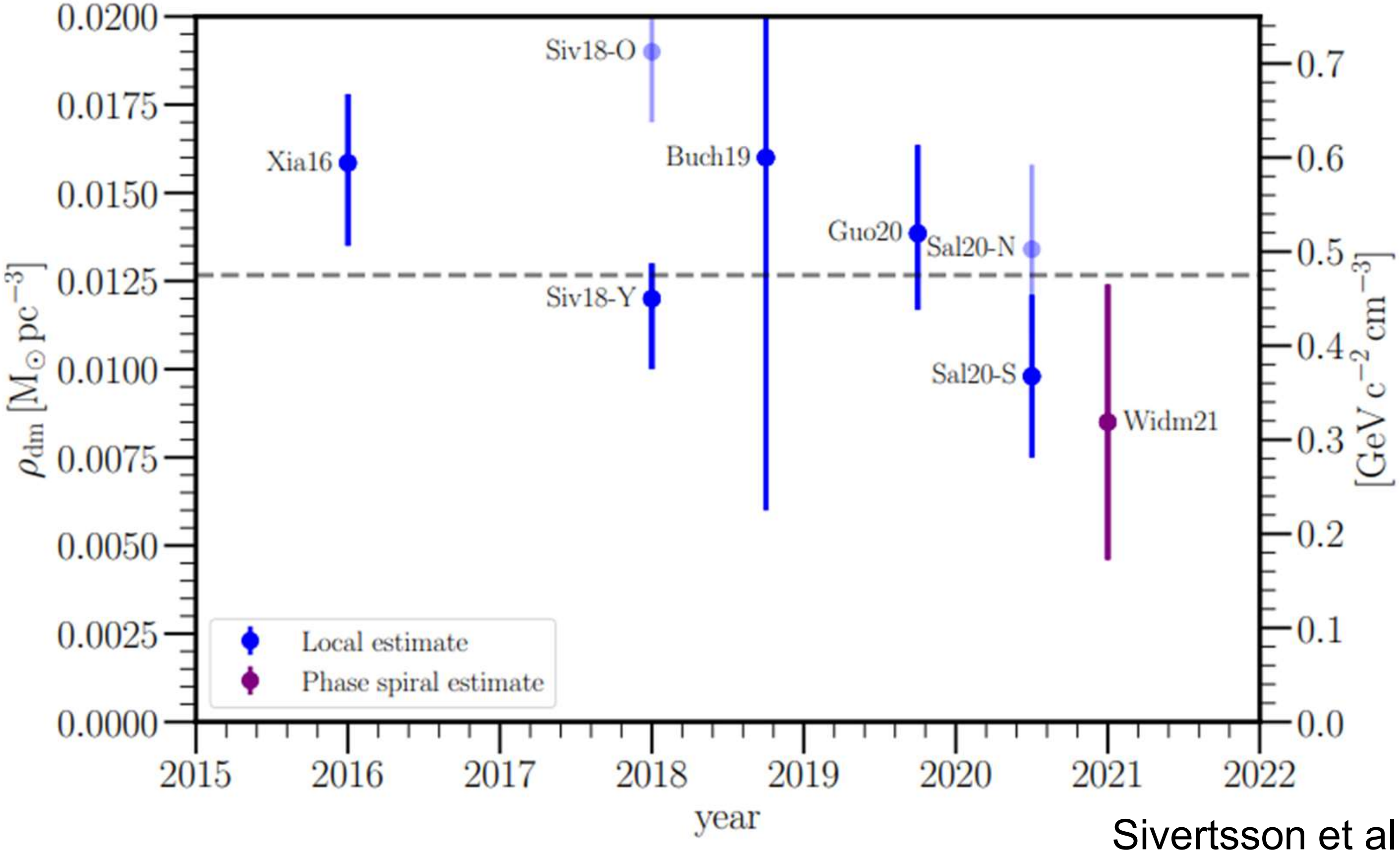

$\simeq$ 0.5 GeV/cm^3

Sivertsson et al. 2022

Evidence for dark matter from rotation curves

Rotation curve of the Milky Way
(Sofue et al. 2009)

$V_{rot}(R)$ (km/s)

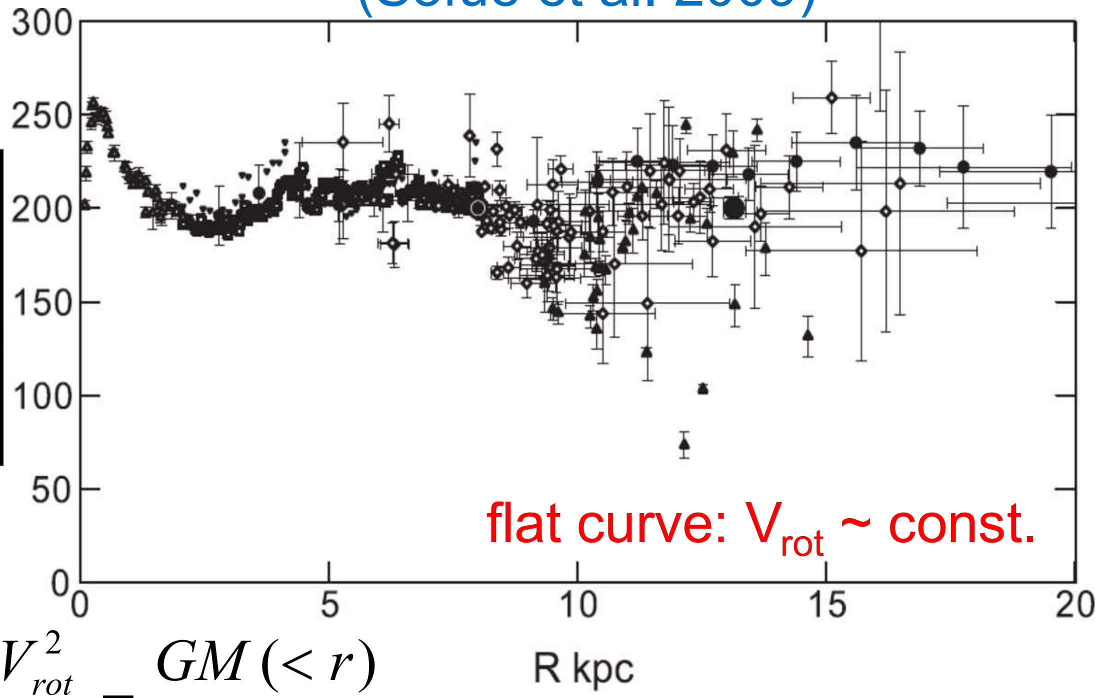

If spherically symmetric, $$\frac{V_{rot}^2}{r} = \frac{GM(<r)}{r^2}$$

$$V_{rot} = const. \Rightarrow M(<r) \propto r$$

Presence of a dark matter halo

Dark matter in an external spiral galaxy

NGC3198

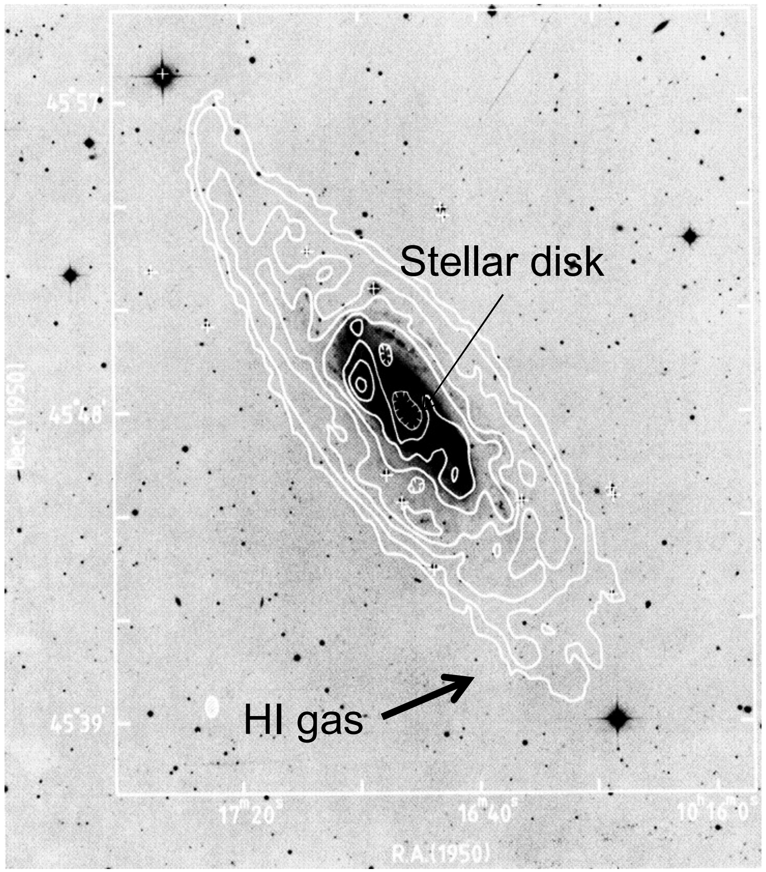

van Albada et al. 1985

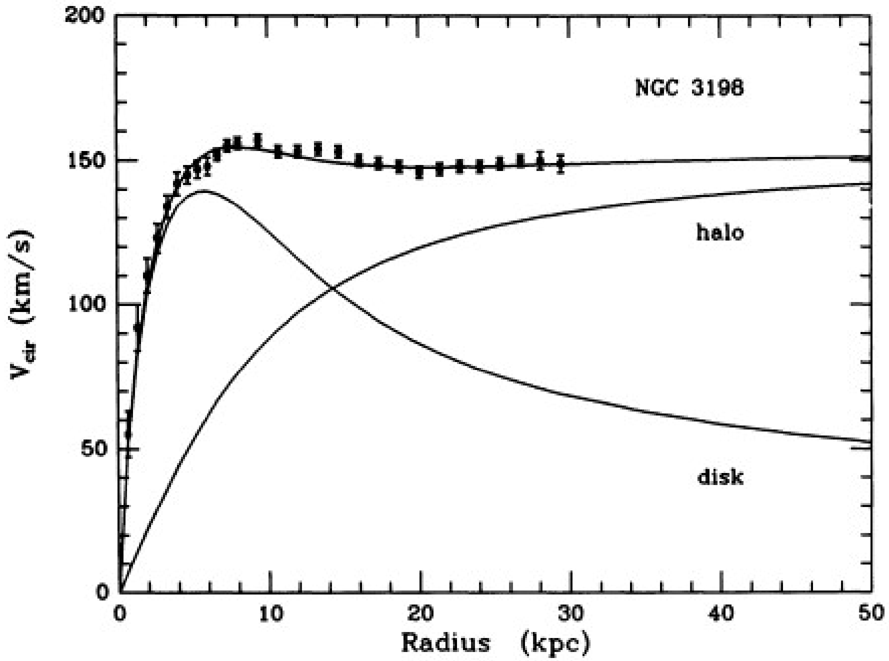

If $\rho(r)$ is spherically symmetric

$V_{rot}(r) = (GM(<r)/r)^{1/2}$

where $M(<r) = \int^r 4\pi\rho r^2 dr$

Dark matter candidates

- Faint compact objects
  - Brown dwarfs, white dwarfs, neutron stars, stellar BHs
  - Primordial BHs
  - MACHOs（Massive Compact Halo Objects ）
- Elementary particles （non-baryonic matter）
  - Neutrino, neutralino, axion…
  - Cold Dark Matter: CDM
    - Massive particles (10~1000 Gev) with small streaming motions
      WIMPs（Weakly Interacting Massive Particles）
      e.g. neutralino
    - Axions

CDM-based structure formation

Distribution of CDM particles → time

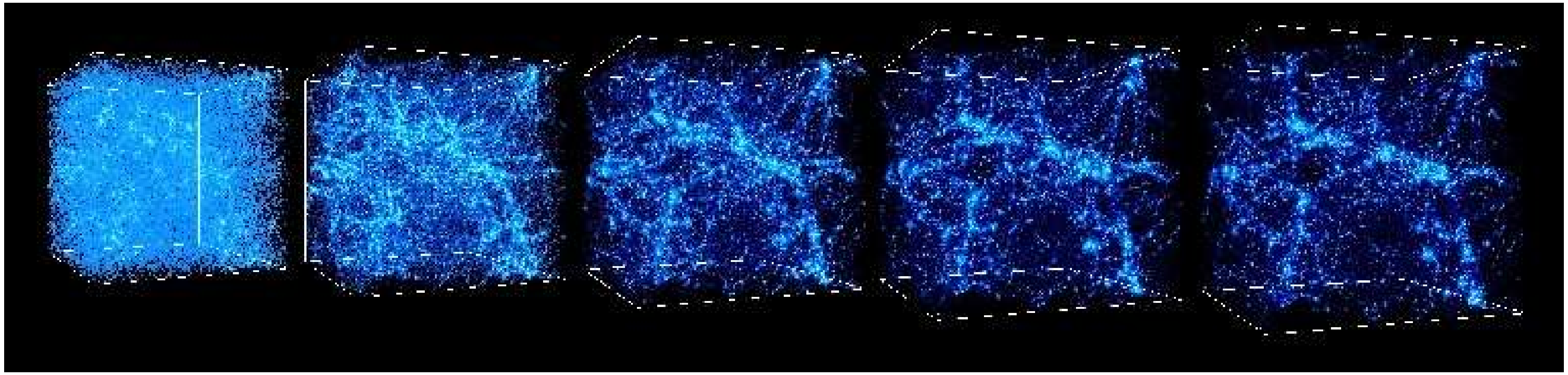

Cold Dark Matter (CDM): WIMP, Axion

Small-scale halos form first, then larger-scale structures form subsequently through merging and accretion

⇒ successful for reproducing observed structures

Density fluctuations in various scales

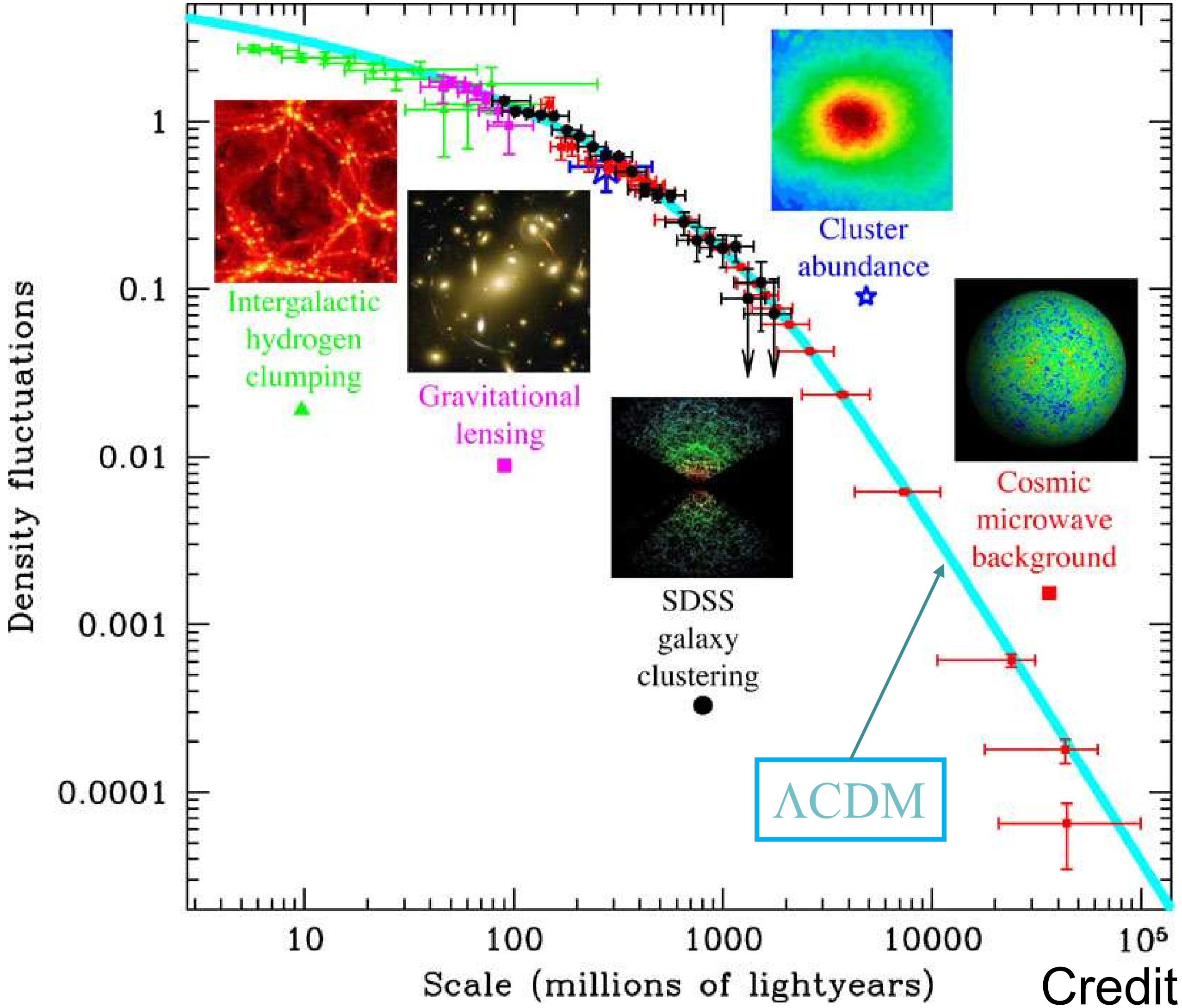

Credit: Tegmark

2. Properties of a dark matter halo
2.1 Total mass

Beyond the rotation curve method

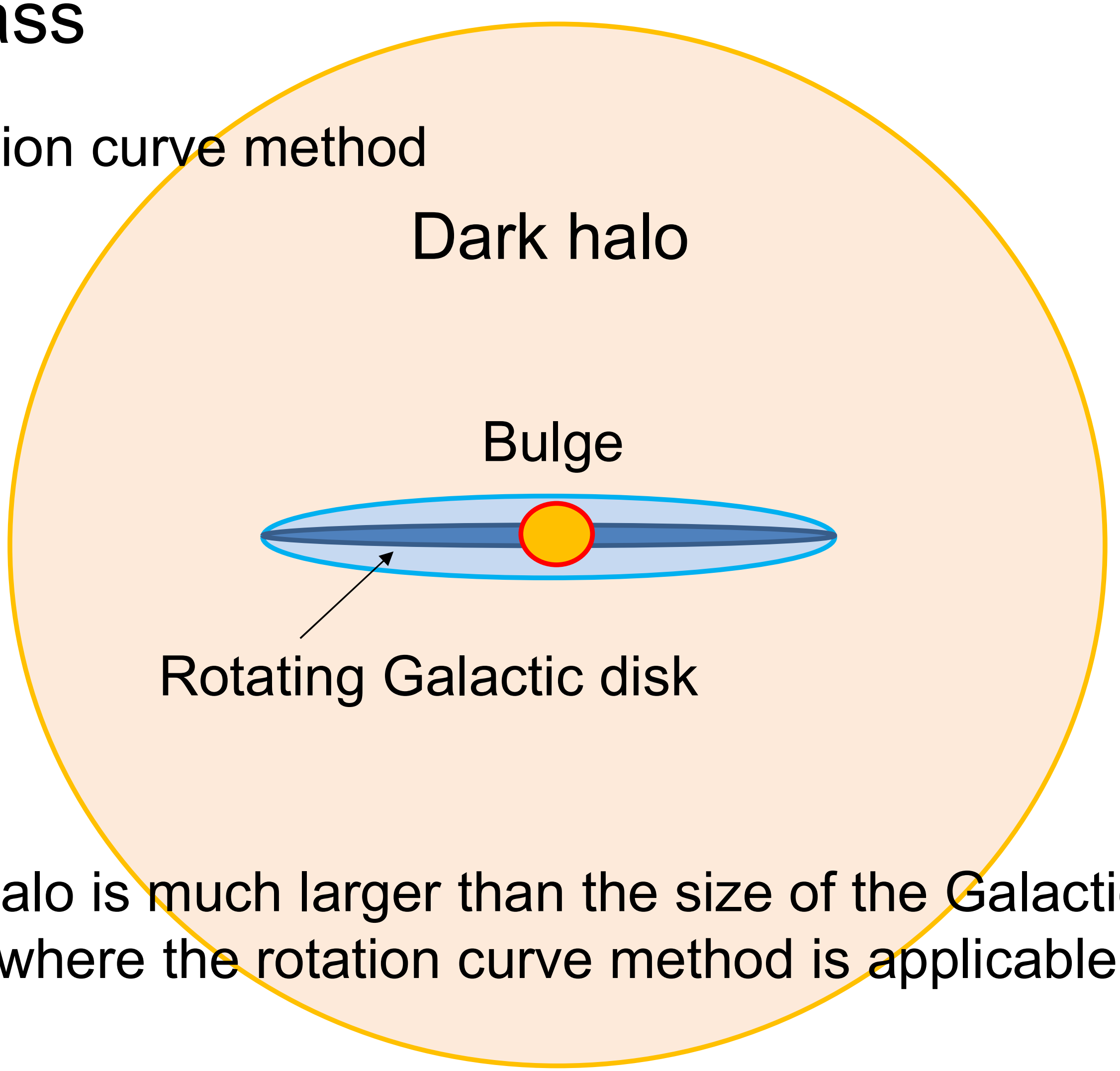

Dark halo is much larger than the size of the Galactic disk, where the rotation curve method is applicable

Halo objects as tracers of dark-halo mass

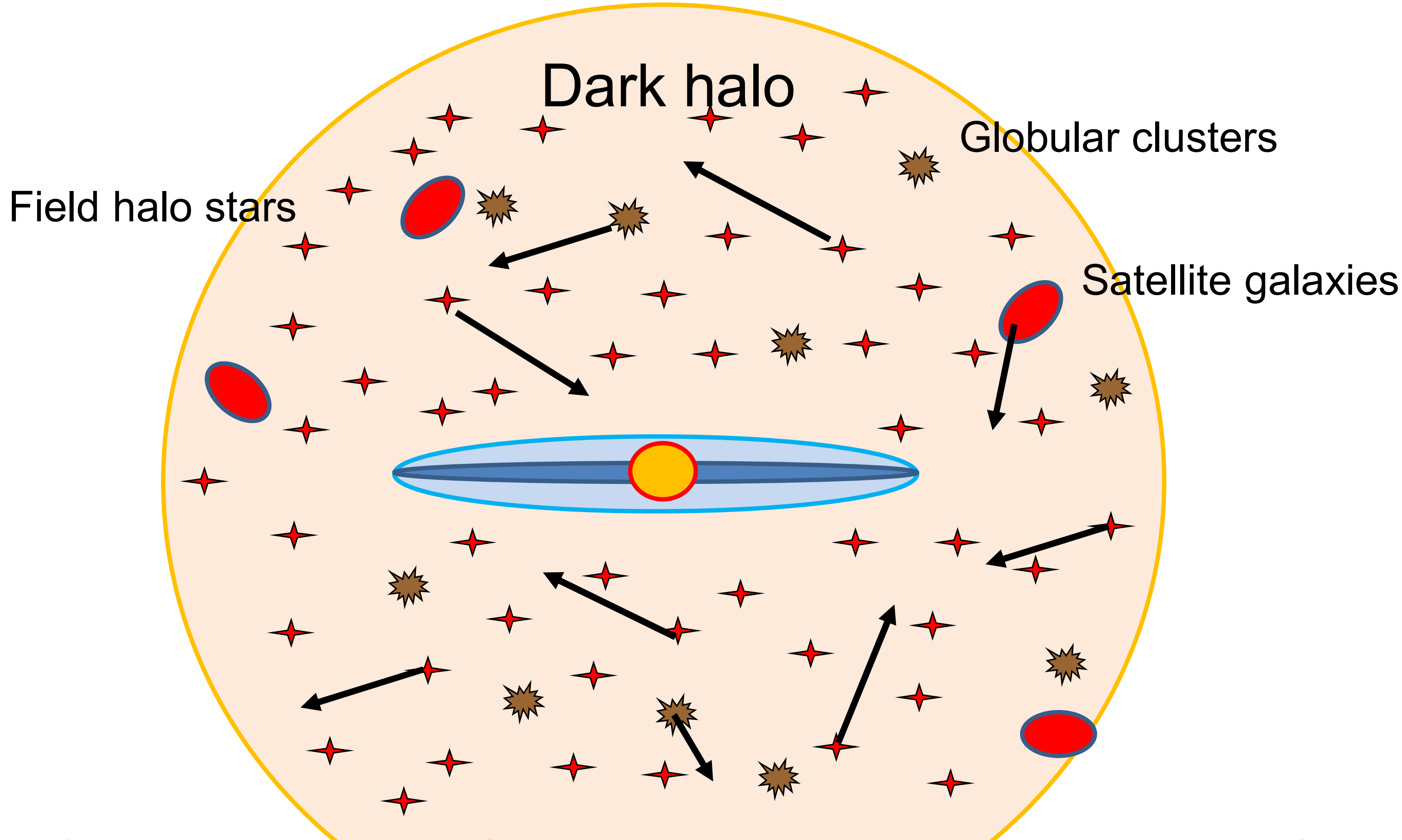

Spatial motions (dominated by random motions) reflect a gravitational potential of a dark halo ⇒ mass

Velocity distribution of disk/halo stars near the Sun

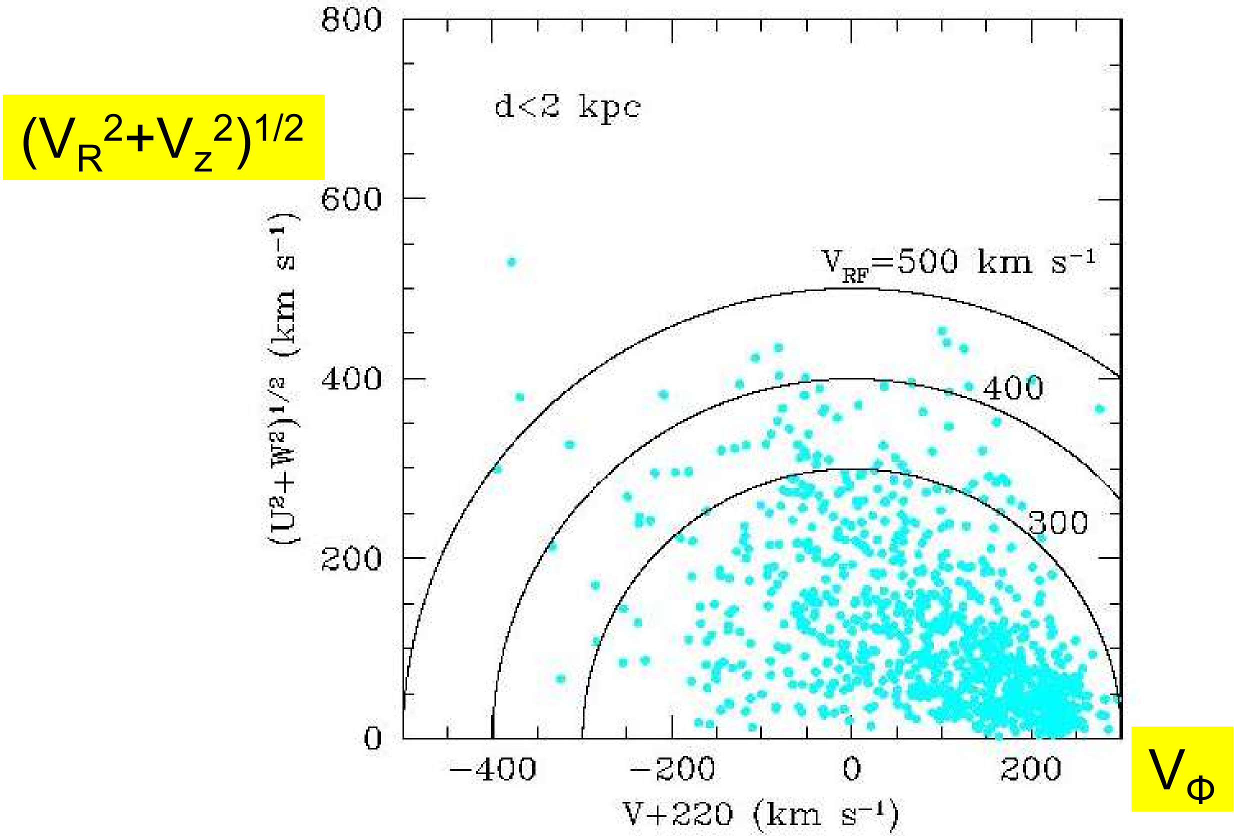

Escape velocity near the Sun: V_{esc}=500~550km/s

⇒ Limits on a gravitational potential Φ at $R=R_{sun}$: $V_{esc}=(2\Phi(R_{sun}))^{1/2}$

Limits on Φ(r) at other radii based on rest-frame velocities of distant sample: $V_{RF} \leq V_{esc}(r)$

(Sakamoto, Chiba, Beers 2003)

$$\Phi(r) = \frac{GM}{a} \log\left(\frac{\sqrt{r^2 + a^2} + a}{r} \right)$$

$$\rho(r) = \frac{M}{4\pi} \frac{a^2}{r^2 (r^2 + a^2)^{3/2}}$$

$\rho \propto r^{-5}$ at $r \gg a$

a: size of a halo

→ total mass M

Case 1 : a = 195 kpc

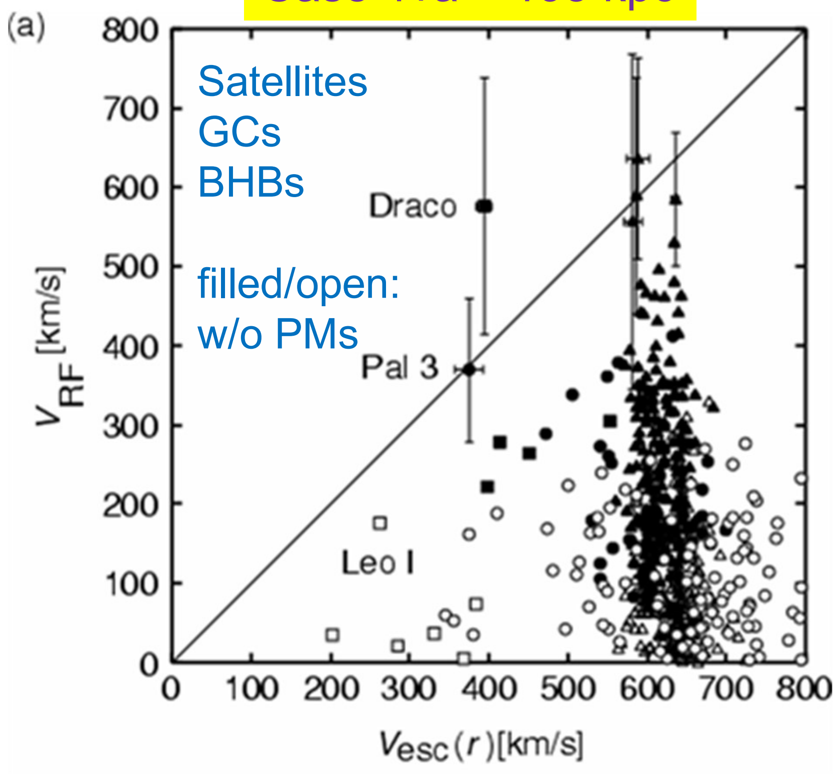

Case 2: a = 20 kpc

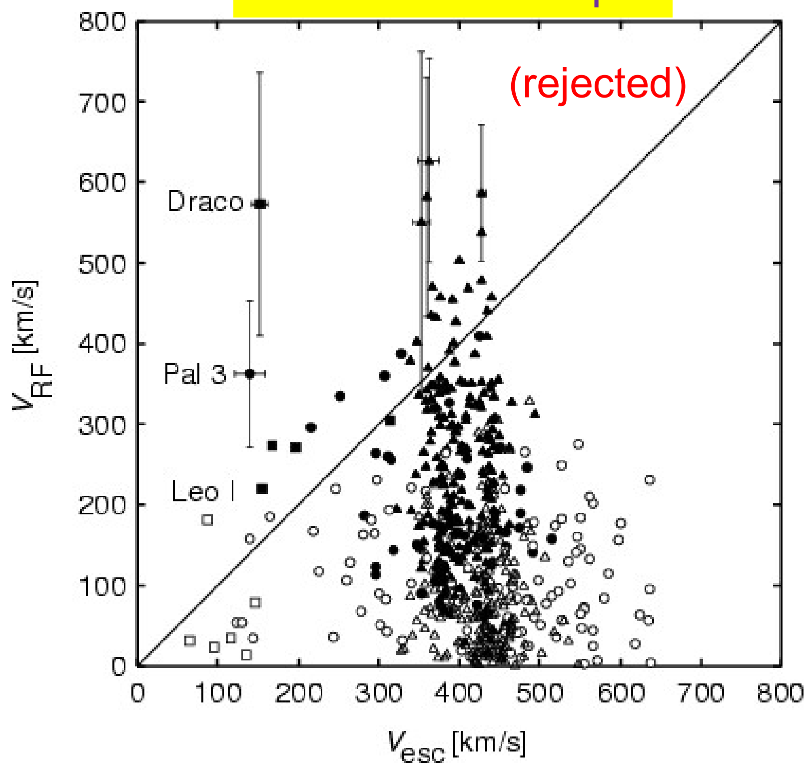

Maximum likelihood method to maximize the probability for getting the observed (r_i, v_i) i=1,N

assumption: stellar distribution function f(E,L)

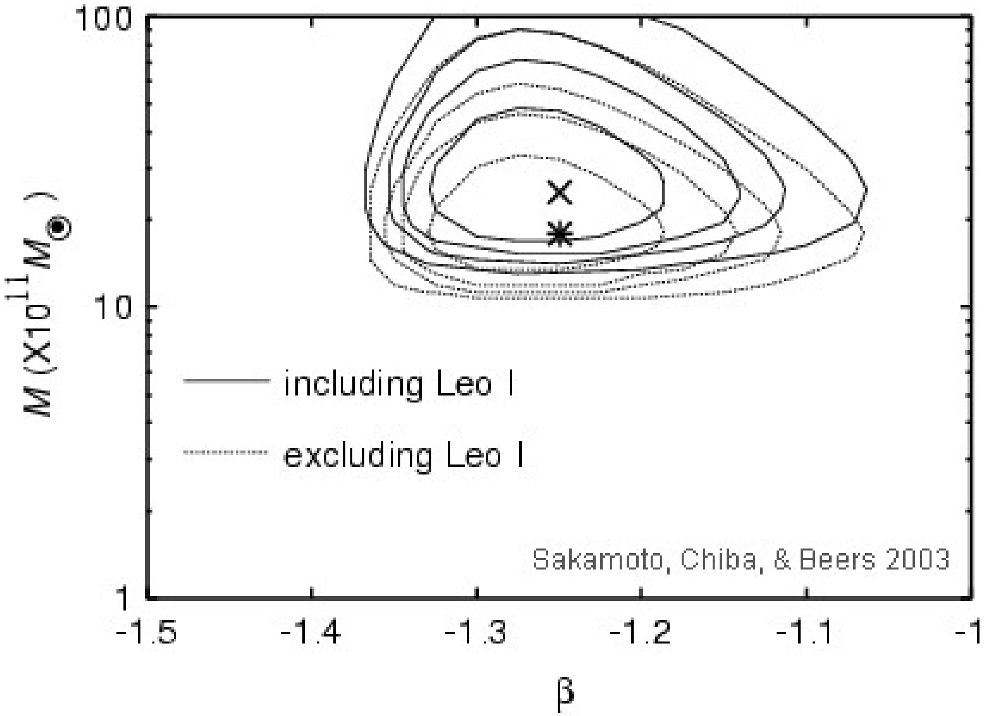

$$\beta = 1 - \frac{\sigma_\theta^2}{\sigma_r^2}$$

Velocity anisotropy parameter

$$\frac{1}{\nu}\frac{d\left(\nu\overline{v_r^2}\right)}{dr} + 2\frac{\beta\overline{v_r^2}}{r} = -\frac{d\Phi}{dr} = -\frac{GM(r)}{r^2}$$

$$\beta = const. \Rightarrow \nu\overline{v_r^2} = r^{-2\beta}\int_r^\infty \frac{\nu GM(r)}{r^2} r^{2\beta} dr$$

Total mass = 2.5 × 10^{12} Msun over ~ 200 kpc
Visible mass = 10^{11} Msun over ~ 15 kpc
⇒ We see only 10 % of the total mass

Recent results using Gaia PMs

Space motions of Globular Clusters

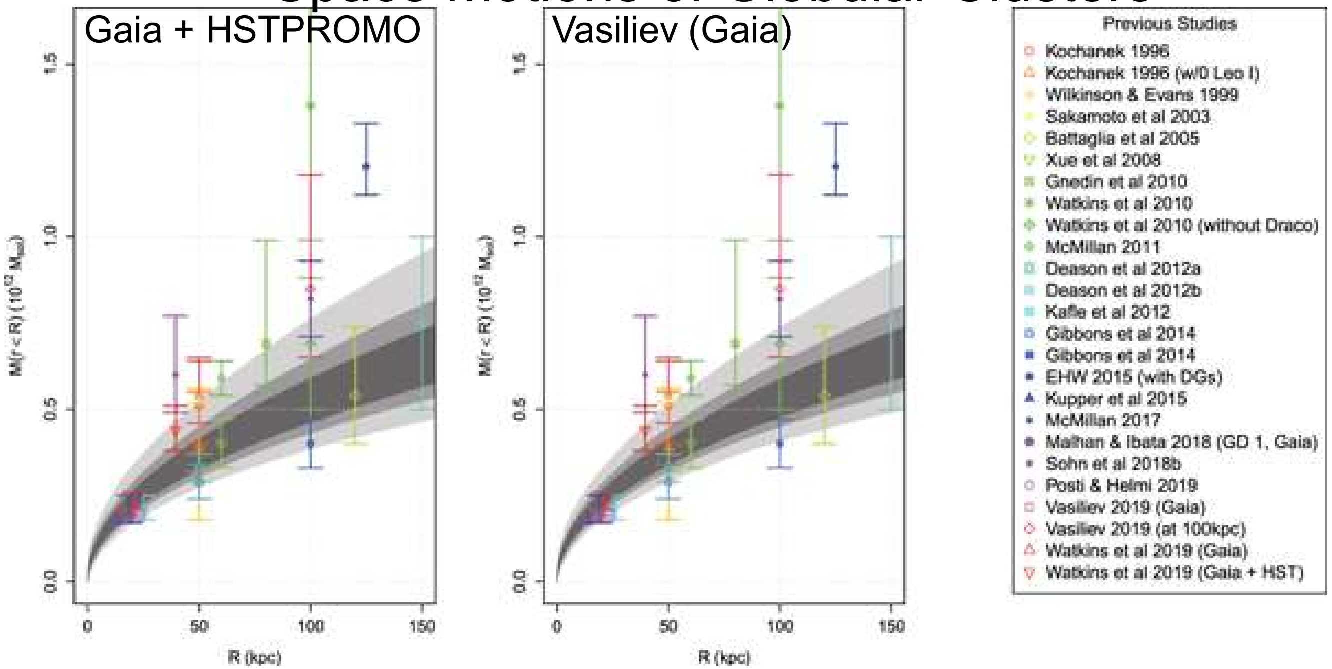

Eadie & Juric 2019 $M_{200} = 0.7^{+0.11}_{-0.08} \times 10^{12}$ Msun (r<200kpc)

Other recent results

Sohn et al. 2018 $M_{vir} = 2.05^{+0.97}_{-0.79} \times 10^{12}$ Msun

Watkins et al 2019 $M_{vir} = 1.41^{+0.99}_{-0.52} \times 10^{12}$ Msun

Posti & Helmi 2019 $M_{vir} = 1.3 \pm 0.3 \times 10^{12}$ Msun

2.2 Global shape

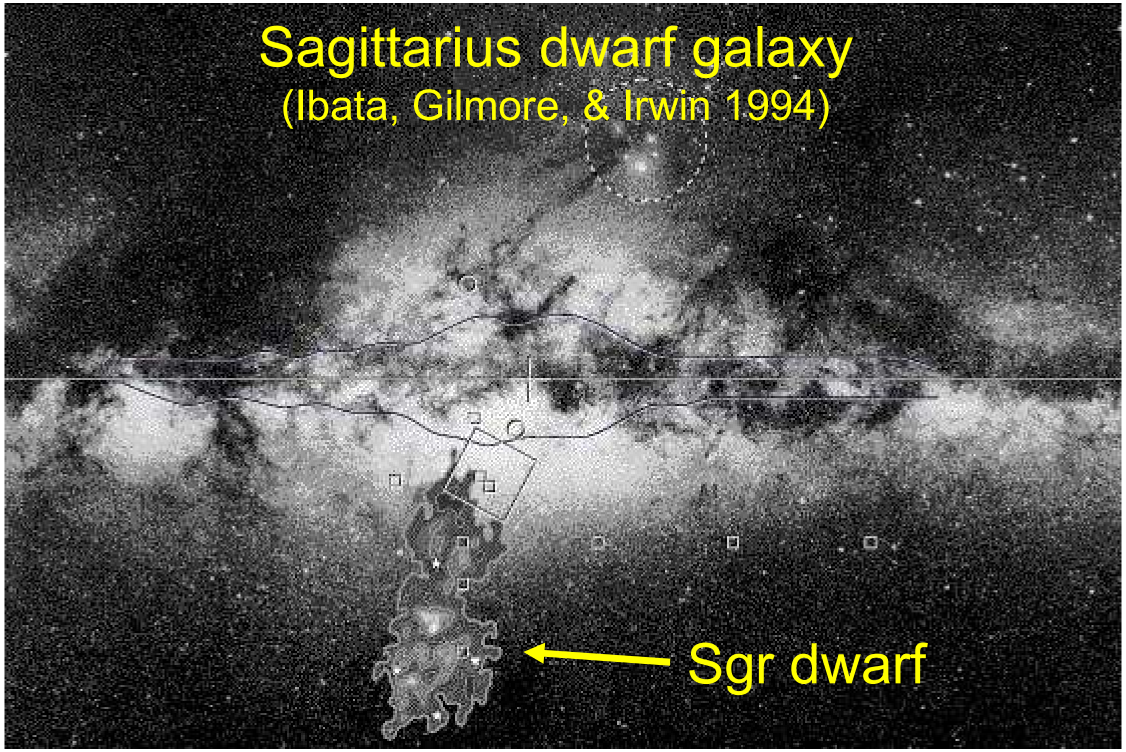

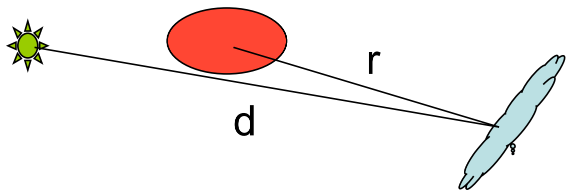

d ~ 24 kpc
r ~ 16 kpc

Sgr stream:
tracer of the MW dark halo

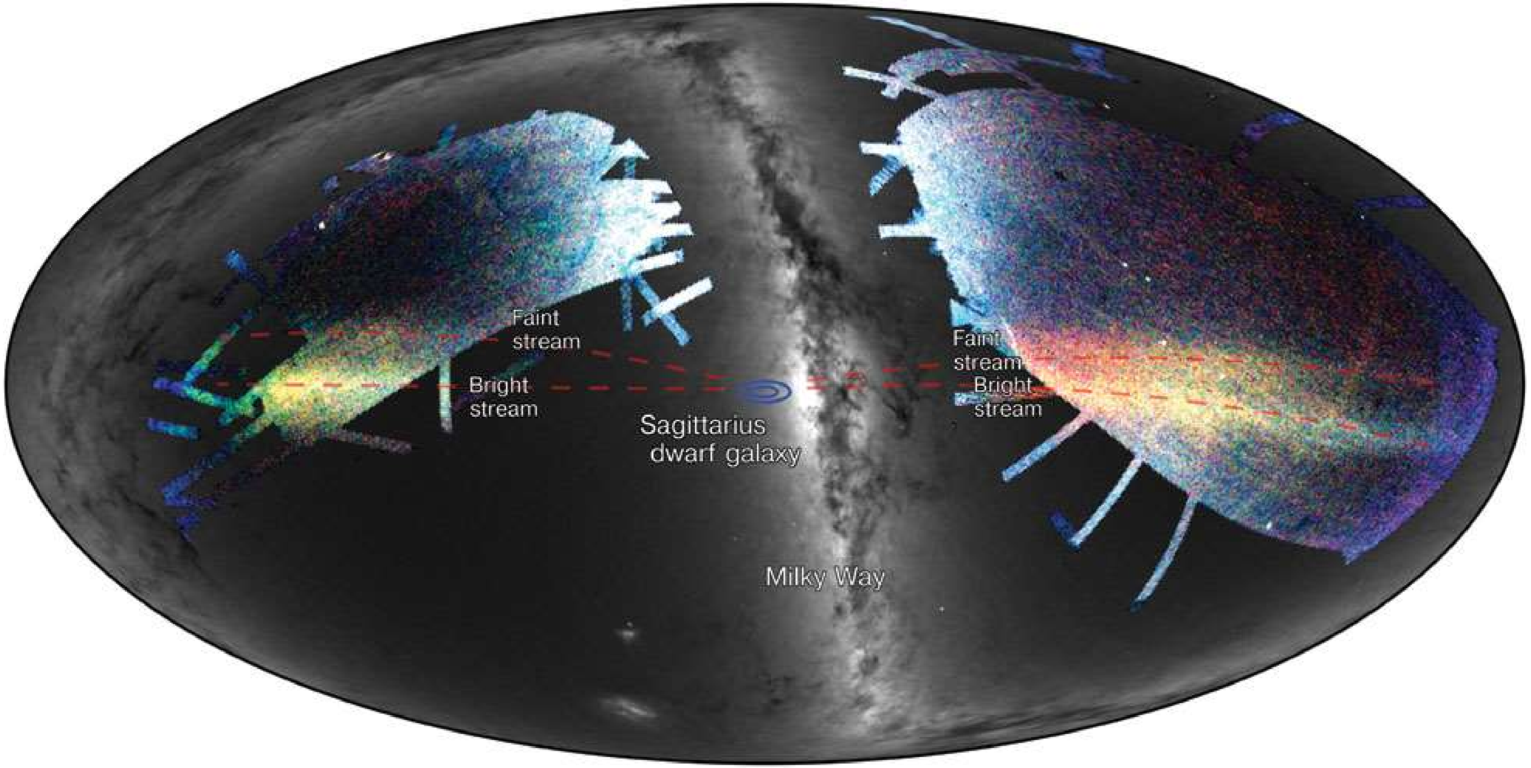

Sgr stream

Majewski et al.

Stream is confined onto an orbital plane
⇒ round dark halo at $15 < r < 60$ kpc

Formation of stellar streams (by tidal force)

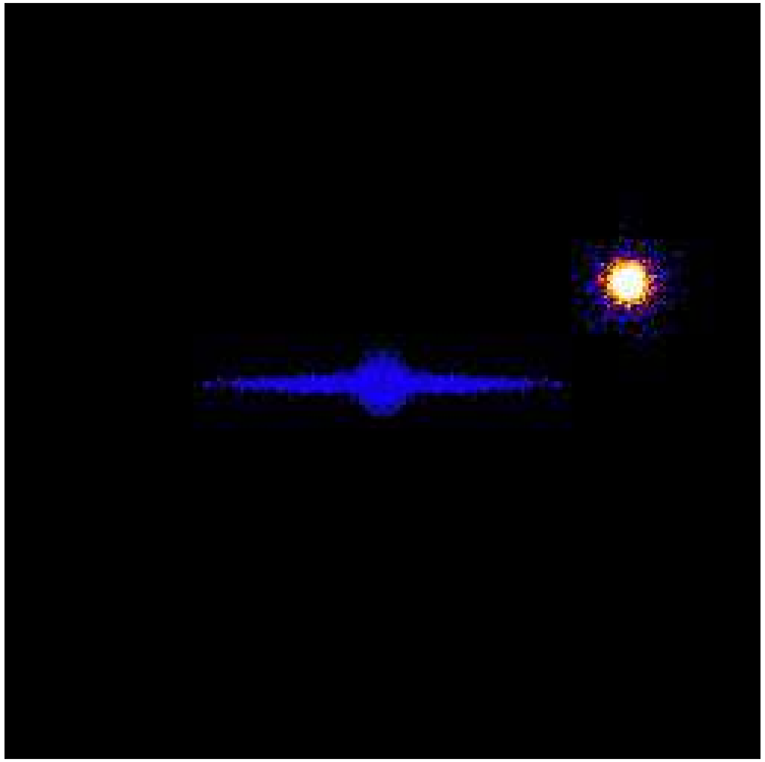

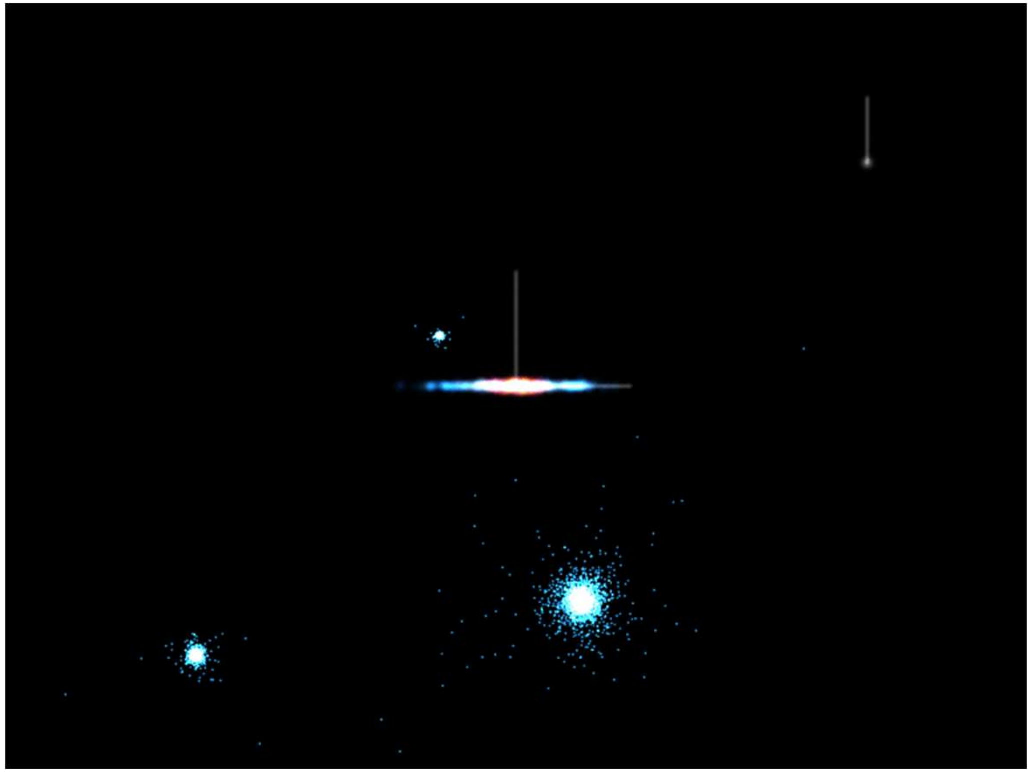

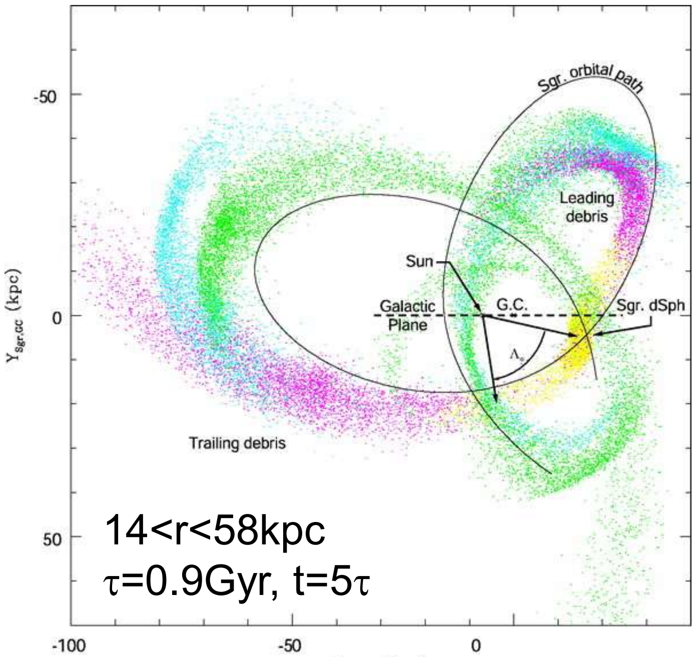

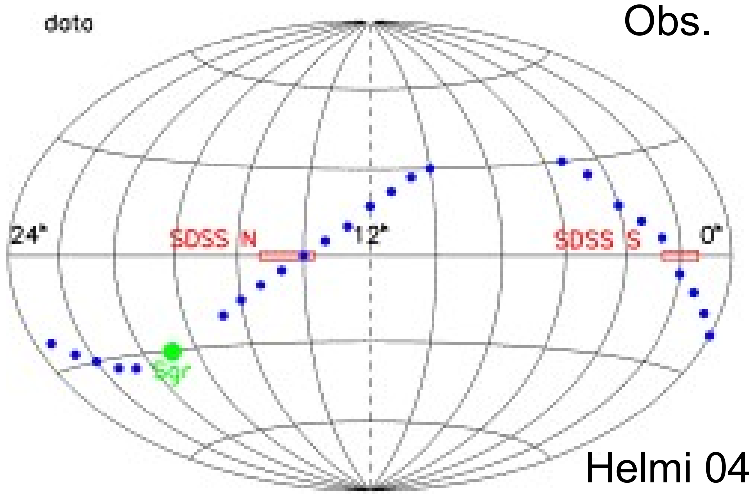

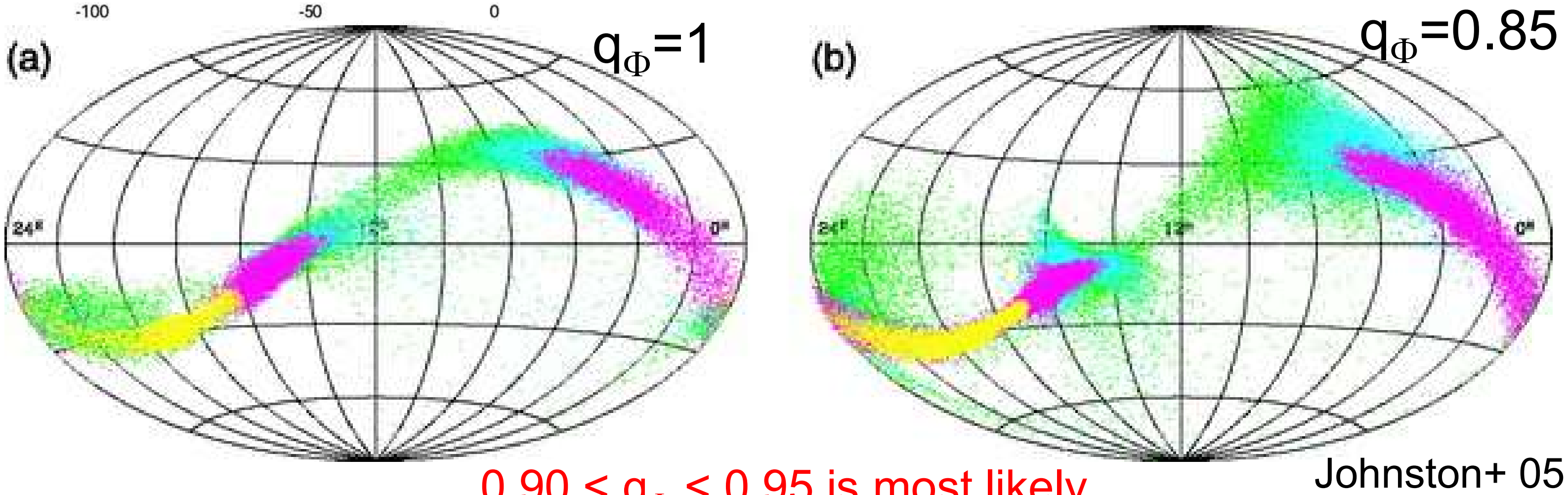

$0.90 < q_\Phi < 0.95$ is most likely

$(0.83 < q_\rho < 0.92)$

However, CDM halos are generally triaxial / prolate.
(Jing & Suto 2000, 2002)

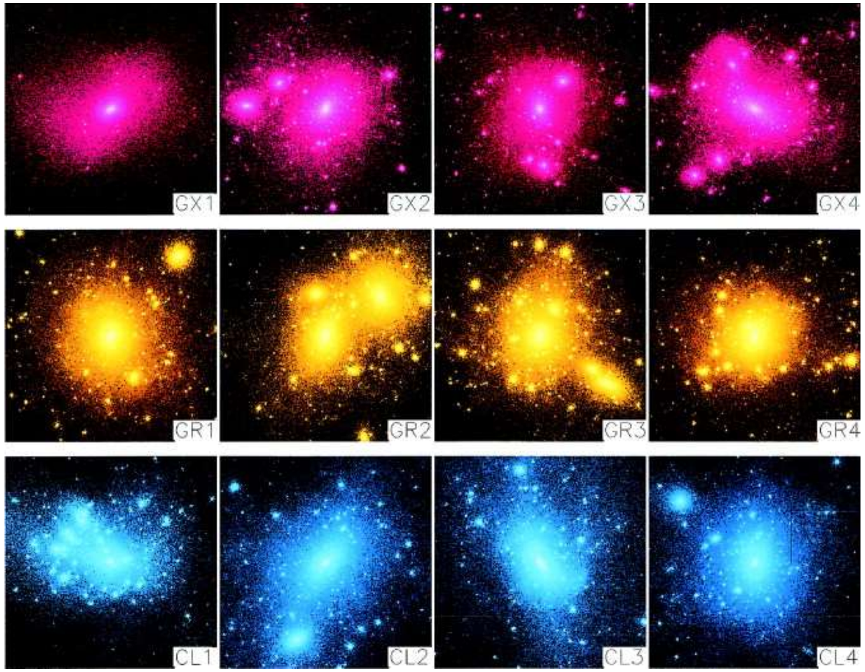

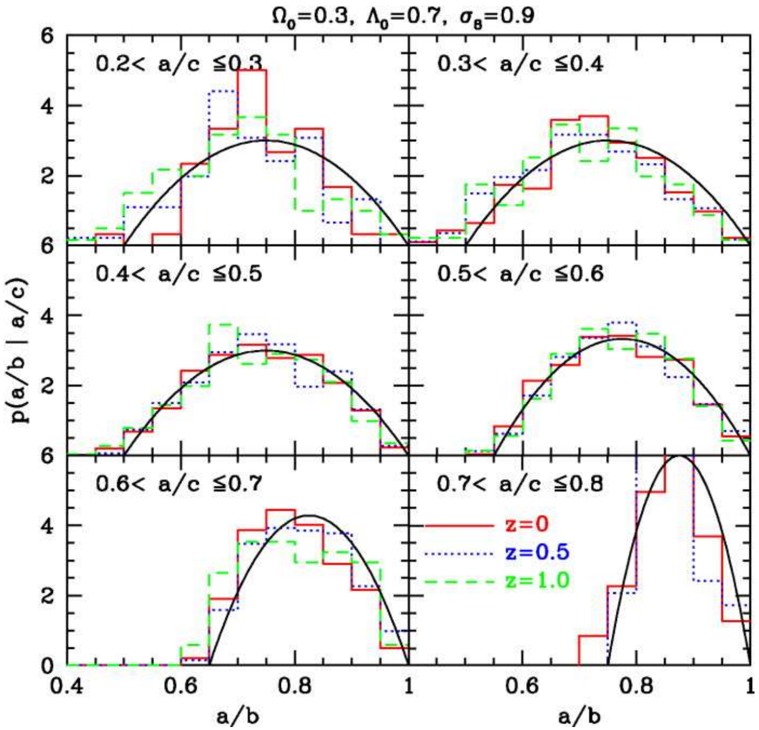

Hayashi+07: $(c/a)_{\Phi}$ = 0.72, $(b/a)_{\Phi}$ = 0.78 in central parts

Gas cooling makes CDM halos rounder

(Kazantzidis et al. 2004)

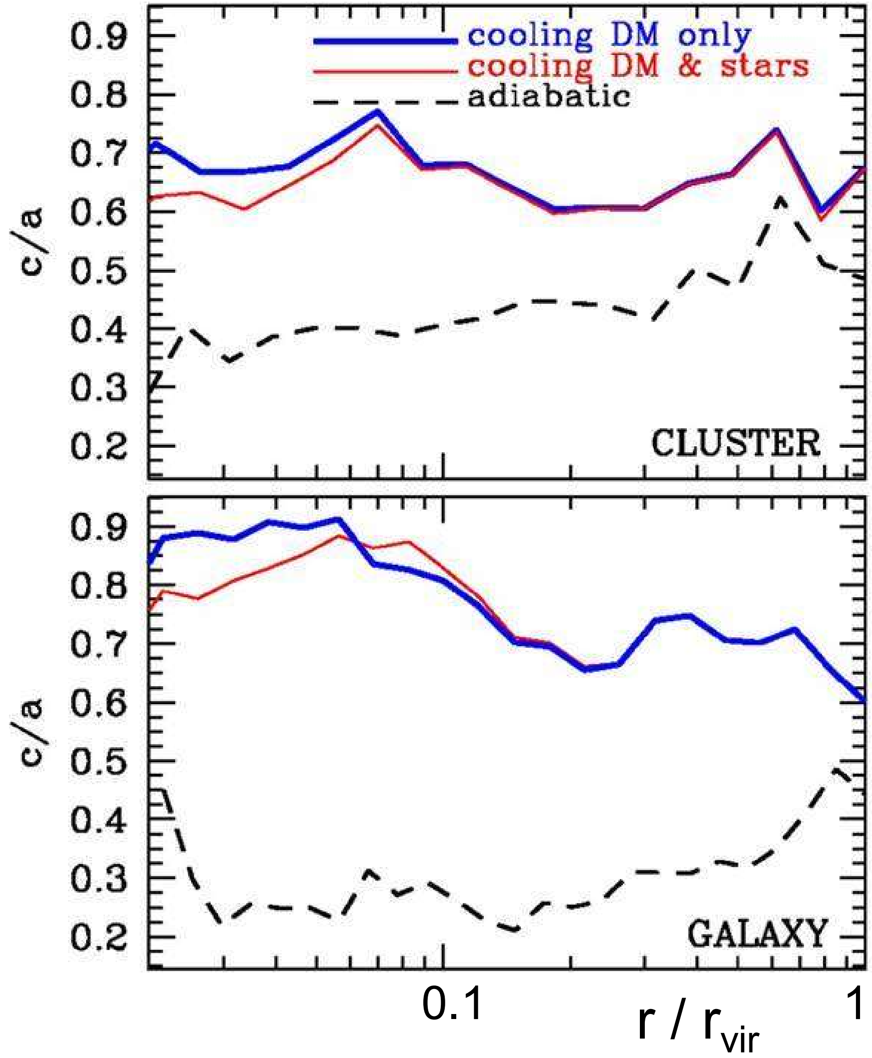

2.3 Density profile

van Albada et al. 1985

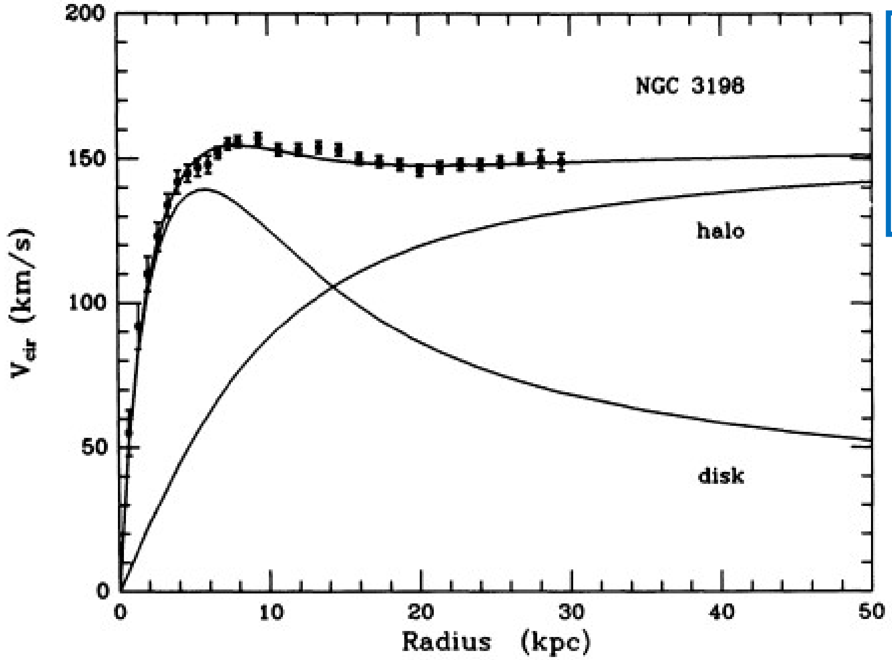

If $\rho(r)$ is spherically symmetric
$V_{rot}(r) = (GM(<r)/r)^{1/2}$
where $M(<r) = \int^r 4\pi\rho r^2 dr$

$V_{rot}(r) = \text{const.}$

$\rho(r) \propto 1 / r^2$
(Singular) isothermal sphere

Prediction of CDM models

Virialized dark halos and their density profiles
(Navarro, Frenk, & White 1997)

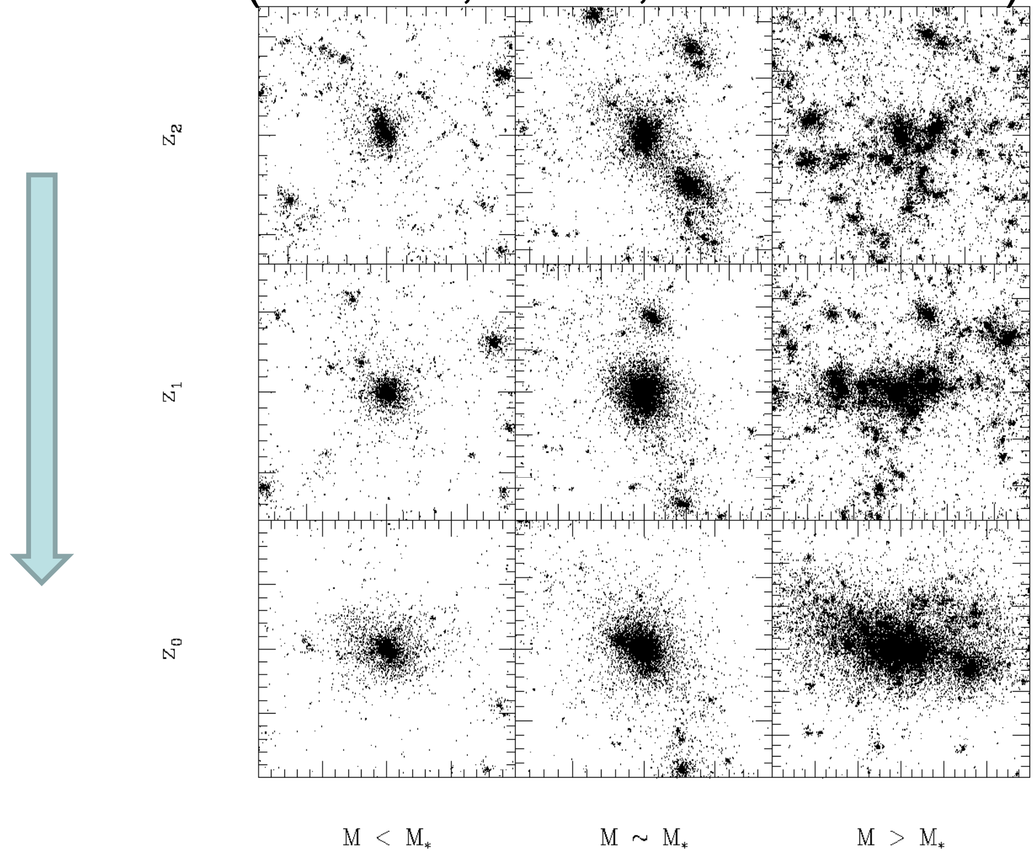

FIG. 1.—Particle plots illustrating the time evolution of halos of different mass in an $\Omega_0 = 1$, $\Lambda = 0$, and $n = -1$ cosmology. The box sizes of each column are chosen so as to include approximately the same number of particles. At $z_0 = 0$, the box size corresponds to about $6r_{200}$. Time runs from top to bottom. Each snapshot is chosen so that M_* increases by a factor of 4 between each row. Low-mass halos assemble earlier than their more massive counterparts. This is true for every cosmological scenario in our series.

NFW profile

$$\rho = \frac{\rho_s}{\left(r/r_s\right)\left(1 + r/r_s\right)^2}$$

$\rho \propto r^{-1}$ at $r << r_s$

$\rho \propto r^{-3}$ at $r >> r_s$

NFW or Moore et al. profile?

(Navarro et al. 2004)

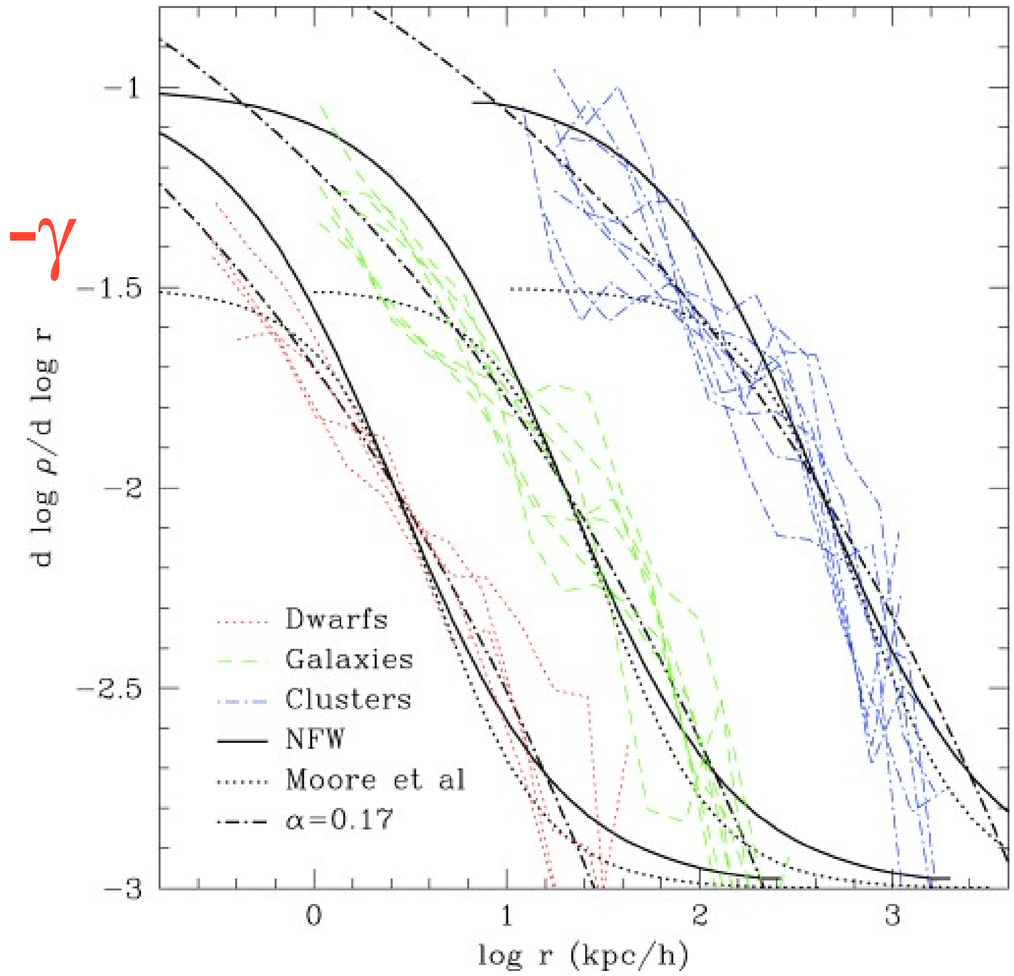

$\rho \propto r^{-\gamma}$
at inner parts
γ= 1: NFW
γ= 1.5: Moore et al.

No universal γ
1 < γ < 1.5

Einasto profile:

$$\ln \rho(r)/\rho_{-2} = (-2/\alpha)\left[(r/r_{-2})^{\alpha} - 1\right]$$

Core/cusp problem

Density distribution of a dark halo

Inner profile: ρ(r) ∝ r^{α}

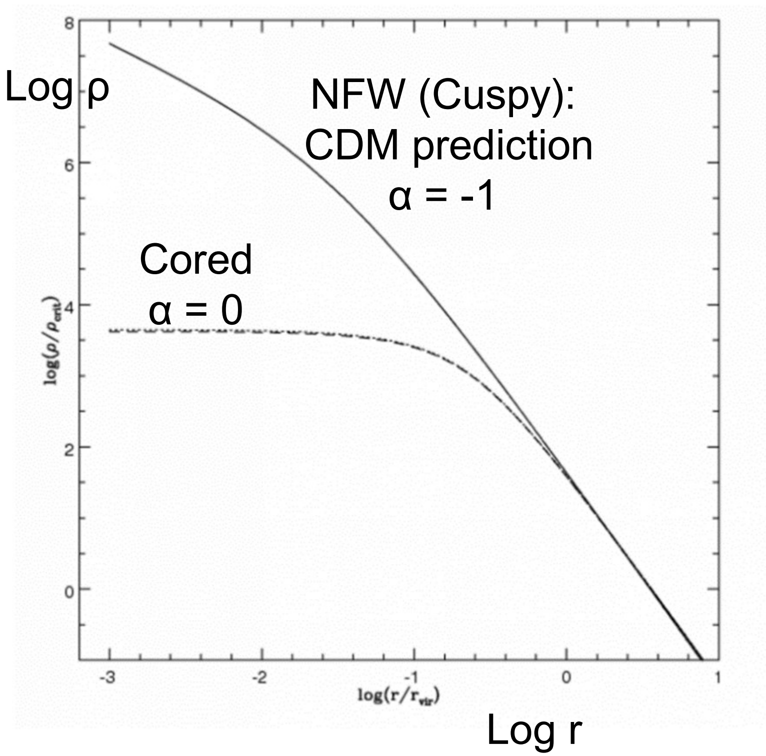

Rotation curves of (external) gas-rich dwarf galaxies

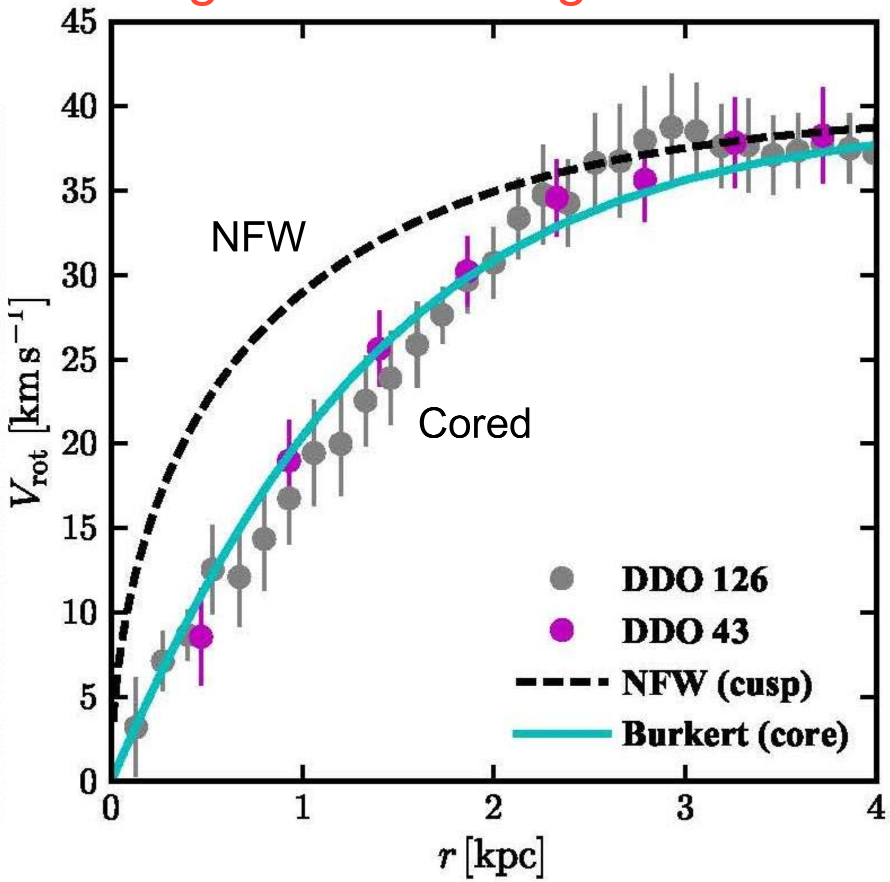

Core/cusp problem

Density distribution of a dark halo

Inner profile: $\rho(r) \propto r^{\alpha}$

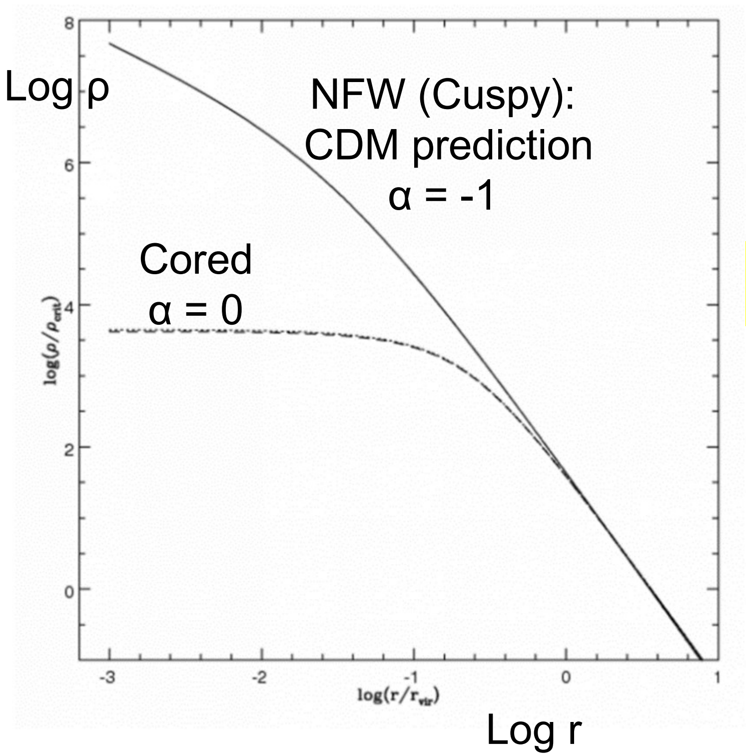

Oh et al. 2015

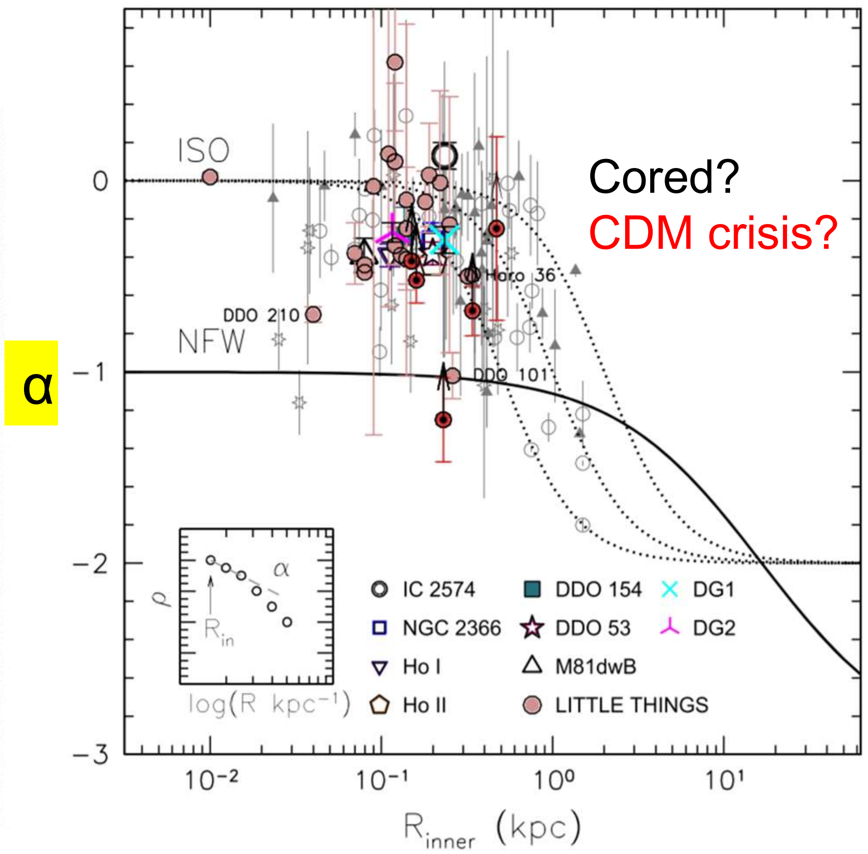

Density profiles of Galactic dwarf spheroidal (dSph) satellites (Walker et al. 2009)

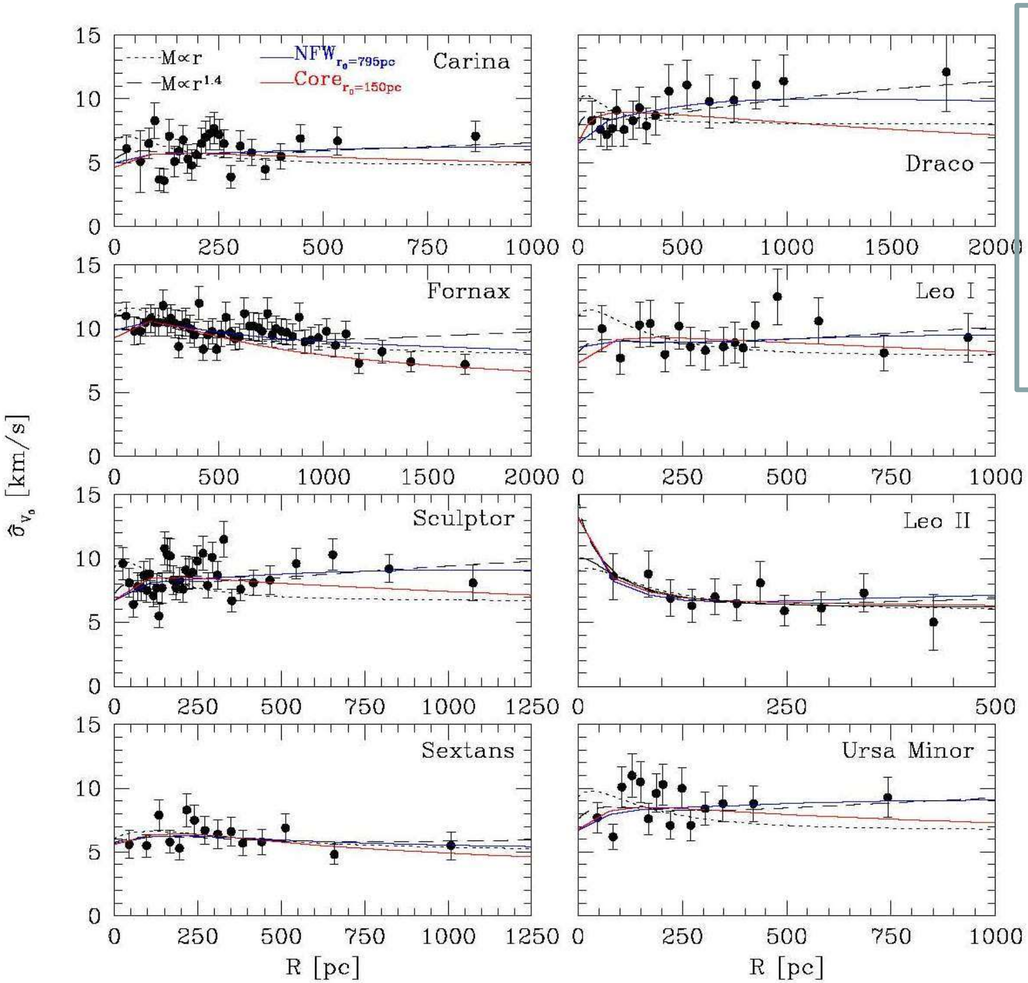

Dark halo model:

$$\rho = \rho_0 \left(\frac{r}{r_0}\right)^{-\gamma} \left[1 + \left(\frac{r}{r_0}\right)^{\alpha}\right]^{\frac{\gamma-3}{\alpha}}$$

NFW: $\gamma=\alpha=1$

Plummer for stars:

$$\nu(r) \propto \left[1 + r^2 / r_h^2\right]^{-5/2}$$

Jeans eq. (spherical sym.)

l-o-s velocity dispersion profile

Some dSphs have core-like profile

Dark matter in the MW satellites

dwarf spheroidal (dSph) galaxies

Sculptor Carina Fornax Leo II Leo I

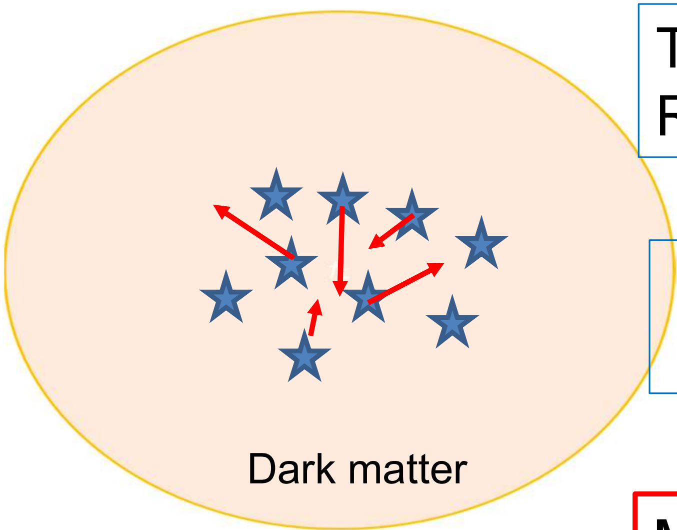

Total stellar mass = $10^4 \sim 10^6 M_{sun}$
Random motion ～10 km/s

↓

Self-gravity of the stellar system alone cannot bind member stars

↓

Massive dark matter needed

Dark matter in the MW satellites

(Mass enclosed within stellar extent ~ 4 x $10^7 M_\odot$)

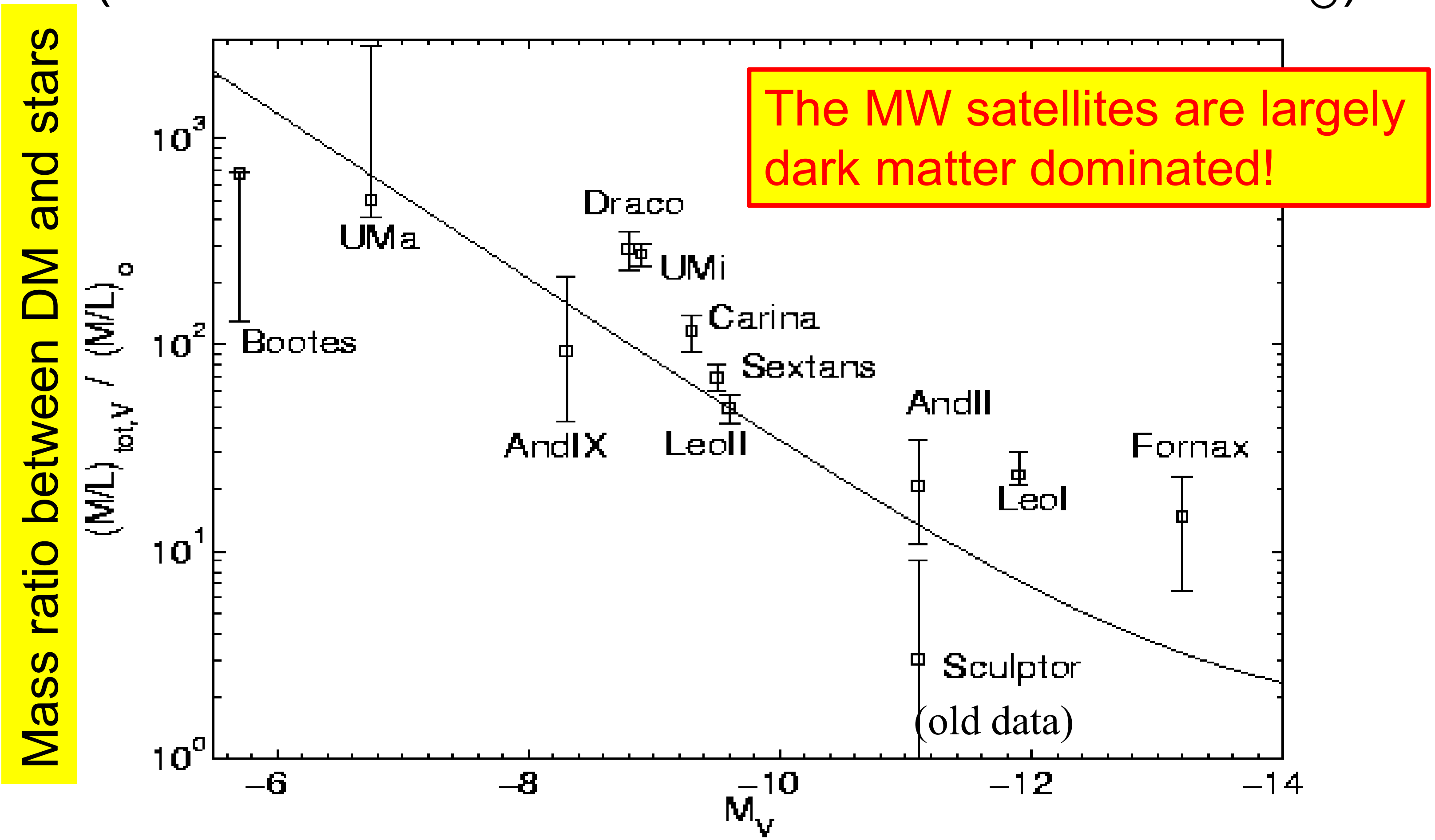

“Too big to fail” problem

Most massive subhalos in ΛCDM simulation are denser than those in most luminous satellites.

Rotation curves of most massive subhalos in the MW-like halos

Filled circles: Galactic satellites rotation velocities at half-light radius

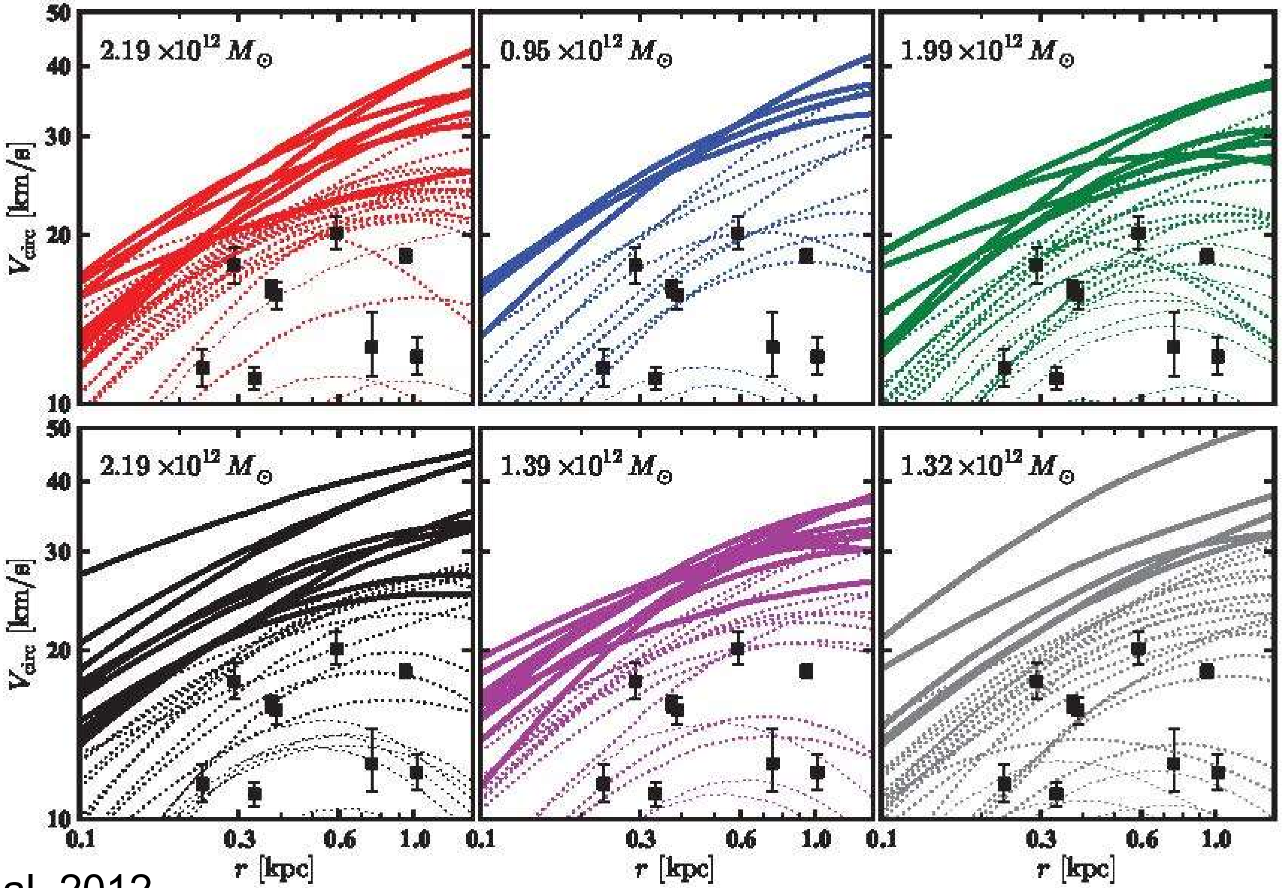

Bolyan-Kolchin et al. 2012

2.4 Substructures

Missing satellites problem

CDM-based simulation result
for the MW-mass halo
(Bullock & Boylan-Kolchin 2017)

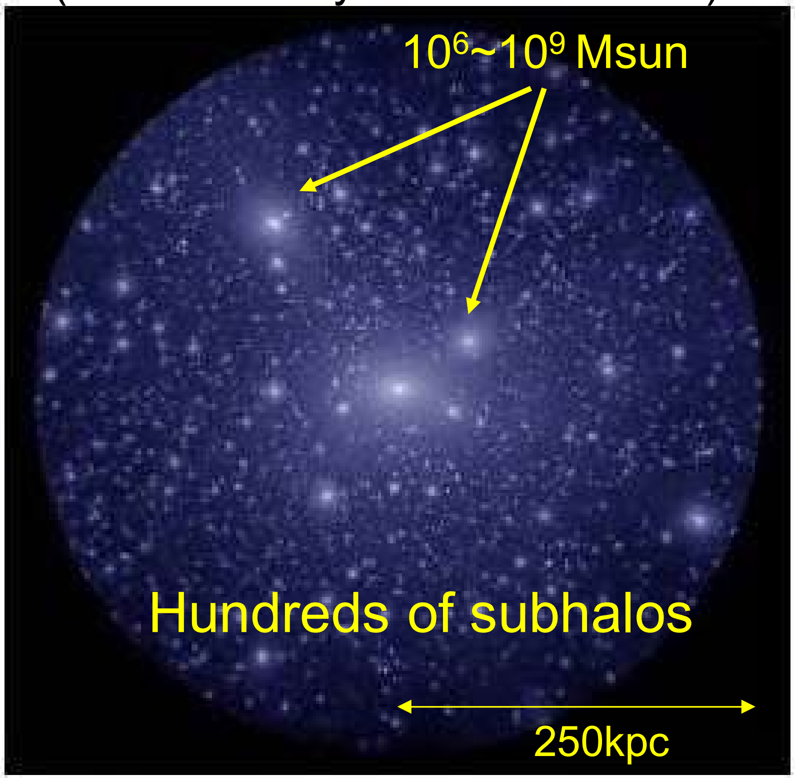

MW satellites

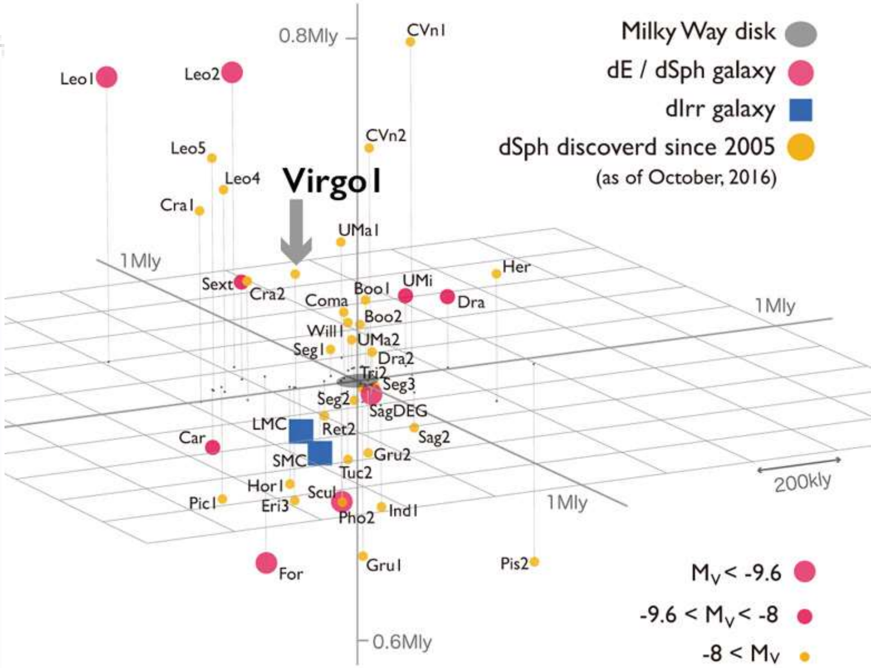

Only ~ 50 satellites are known

Power spectrum for DMs

BB-K2017

$$\Delta^2(k) \propto \frac{k^3}{2\pi} P(k)\, T^2(k)$$

Dark halos on scales of dwarf galaxies are most important keys

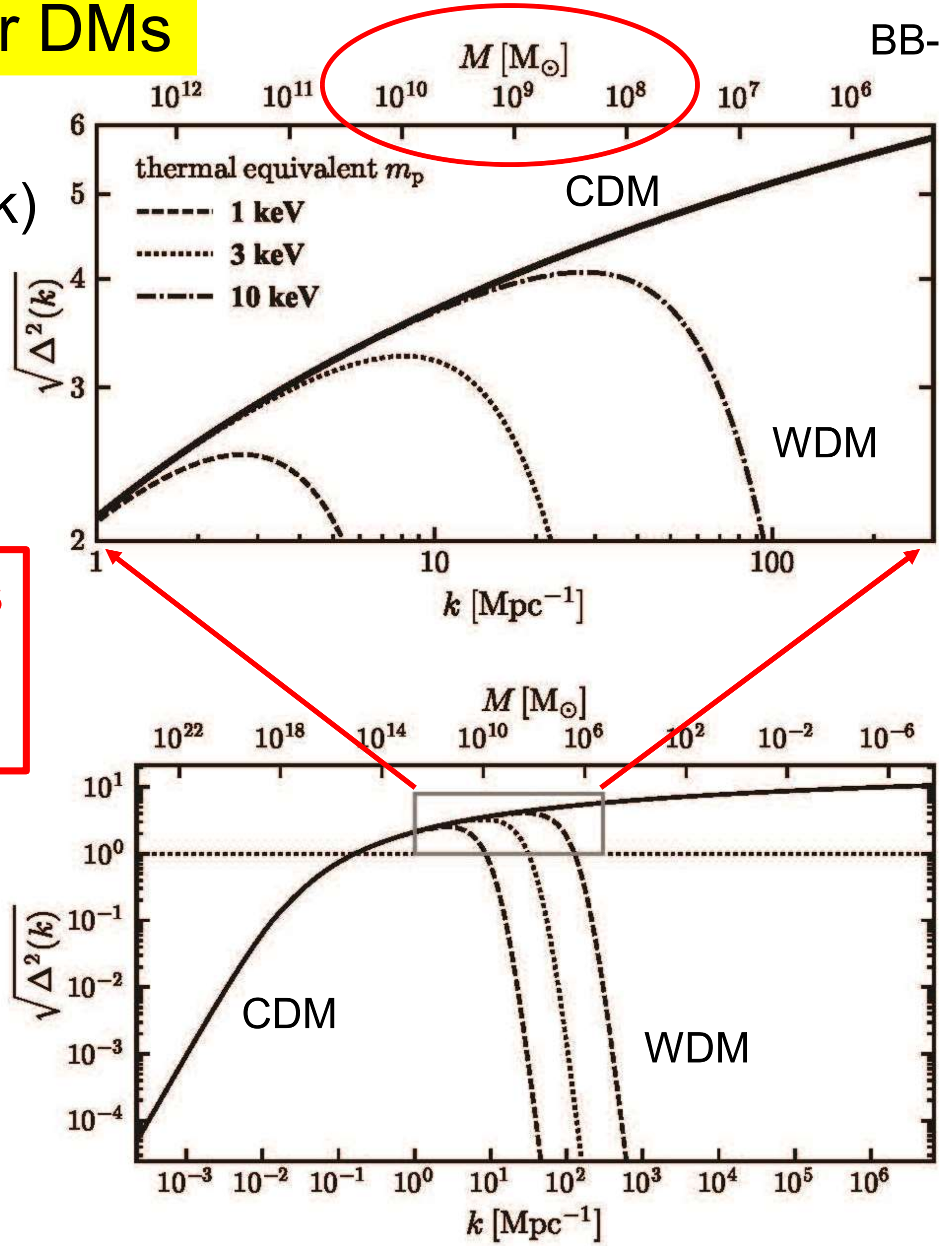

Alternative dark matter models

- Self-Interacting DM (SIDM)
  Interaction among DM particles
  cross section: σ/m
  Cored profile is reproduced
- Warm Dark Matter (WDM)
  m ~ O(keV) e.g. sterile neutrino
  Number of subhalos is reduced

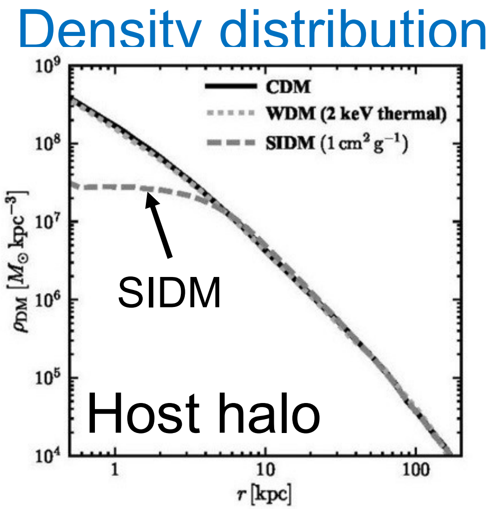

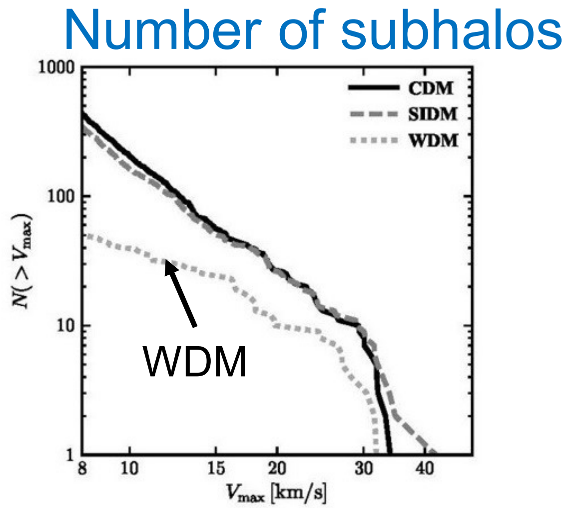

Various dark matter candidates

Ferreira 2020

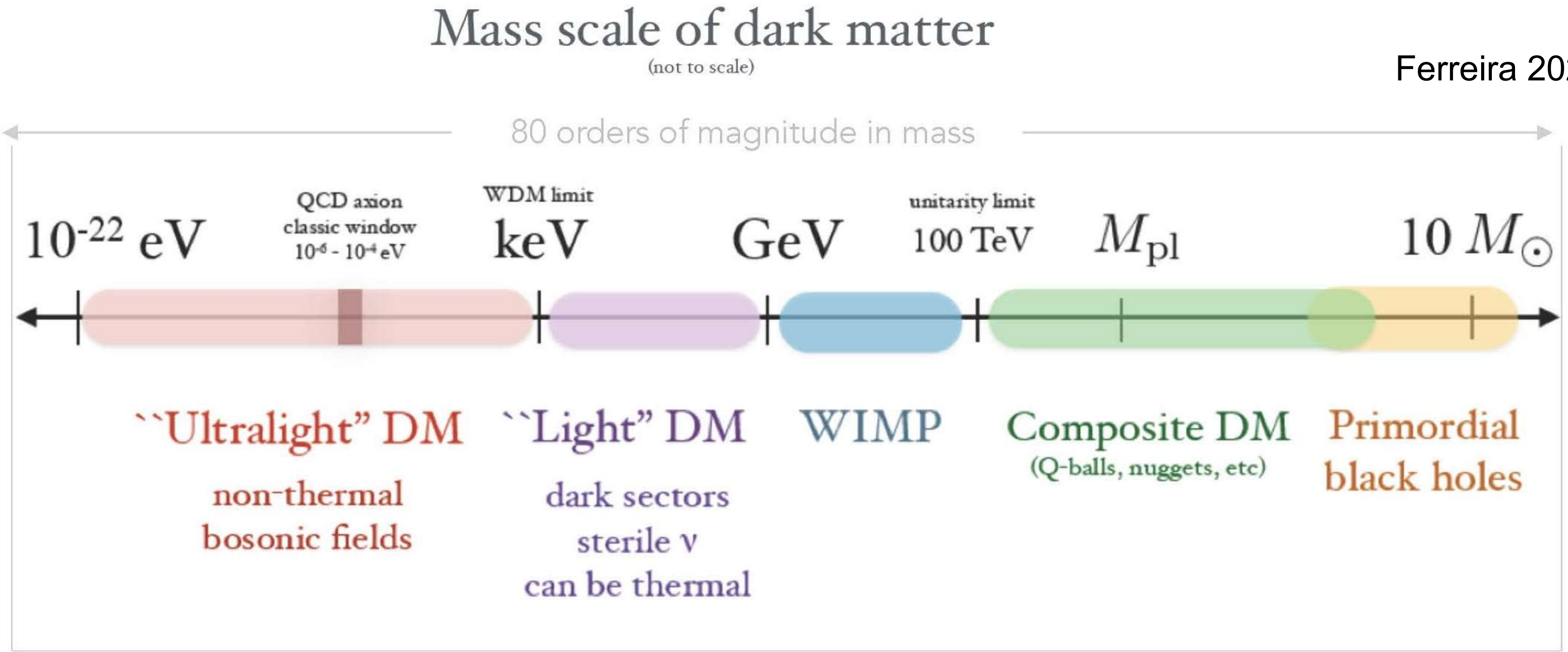

Unsolved big issue!

Ultralight DM：Fuzzy Dark Matter (FDM)

Hu, Barkana, Gruzinov (2000)

Jowett Chan

$m = 1 \times 10^{-22}$ eV

Chan, Ferreira, May, Hayashi, Chiba (2022)

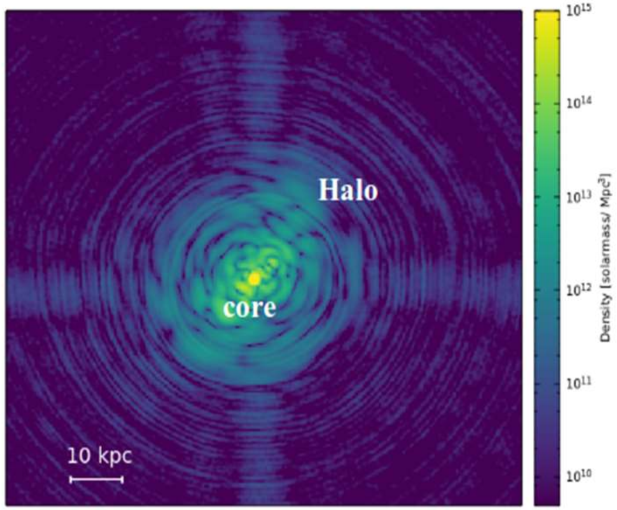

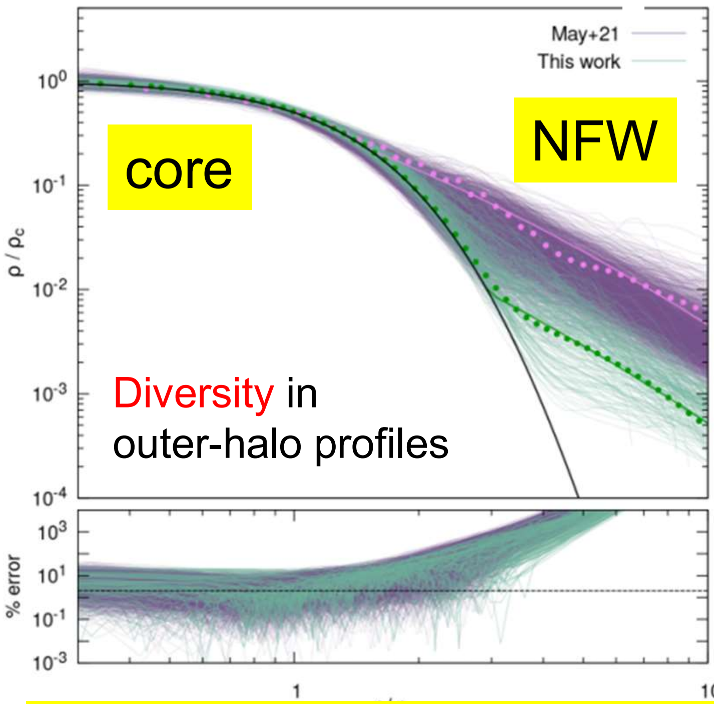

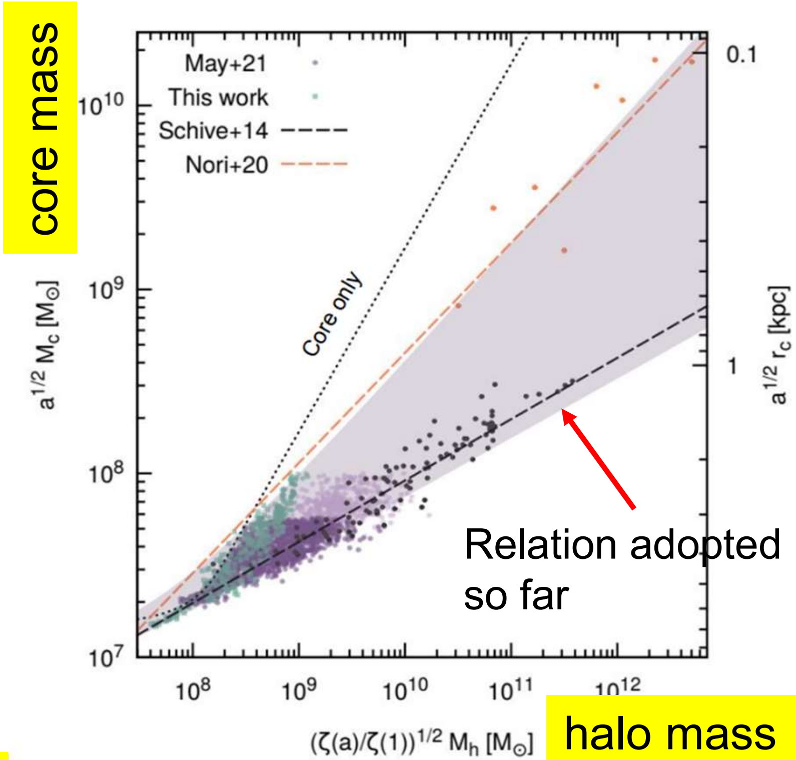

Quantum pressure vs. gravity

$$\lambda_J = 55 \left(\frac{m}{10^{-22}\mathrm{eV}}\right)^{-1/2} \left(\frac{\rho}{\bar{\rho}}\right)^{-1/4} (\Omega_m h^2)^{-1/4}\ \mathrm{kpc}$$

A few kpc scales: dwarf galaxy sales

$$\rho_{\rm soliton}(r) = \frac{1.9 \times 10^{12} M_\odot\ \mathrm{pc}^{-3}}{[1 + 0.091(r/r_c)^2]^8} \left(\frac{m_\psi}{10^{-22}\mathrm{eV}}\right)^{-2} \left(\frac{r_c}{\mathrm{pc}}\right)^{-4}$$

Diversity in core-halo mass relationship is discovered.

Probing dark matter substructures

- Dynamical effects on galactic structure
  - Star clusters and stellar streams
  - Stellar disks
- Effects on gravitational lensing
  - Anomalous flux ratios between lensed images
  - Effects on extended lensed images

Probing evidence for CDM subhalos from their gravitational effects on a stellar stream

(Carlberg 2011)

CDM halo in a galaxy

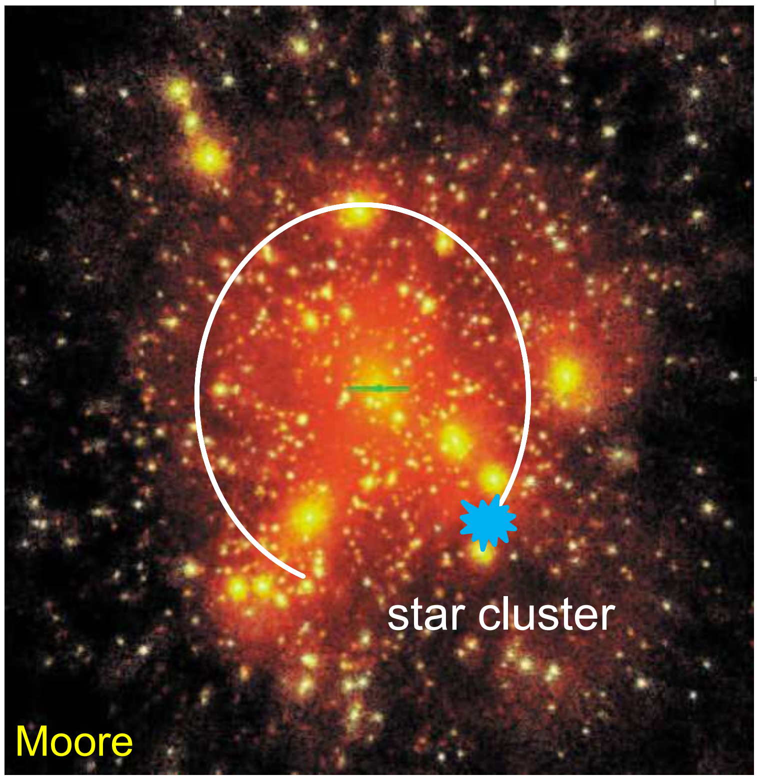

dynamical effects on stellar stream ($M_{star}=10^6 M_{sun}$

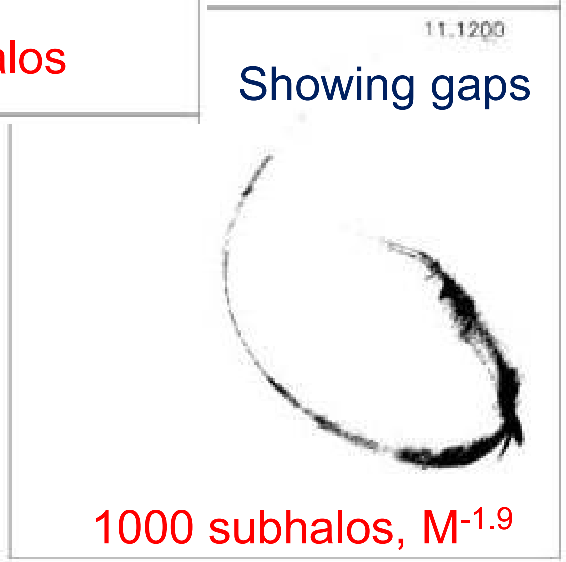

Perturbation in the MW stream

Bonaca et al. 2019 GD-1 stream selected with Gaia PMs

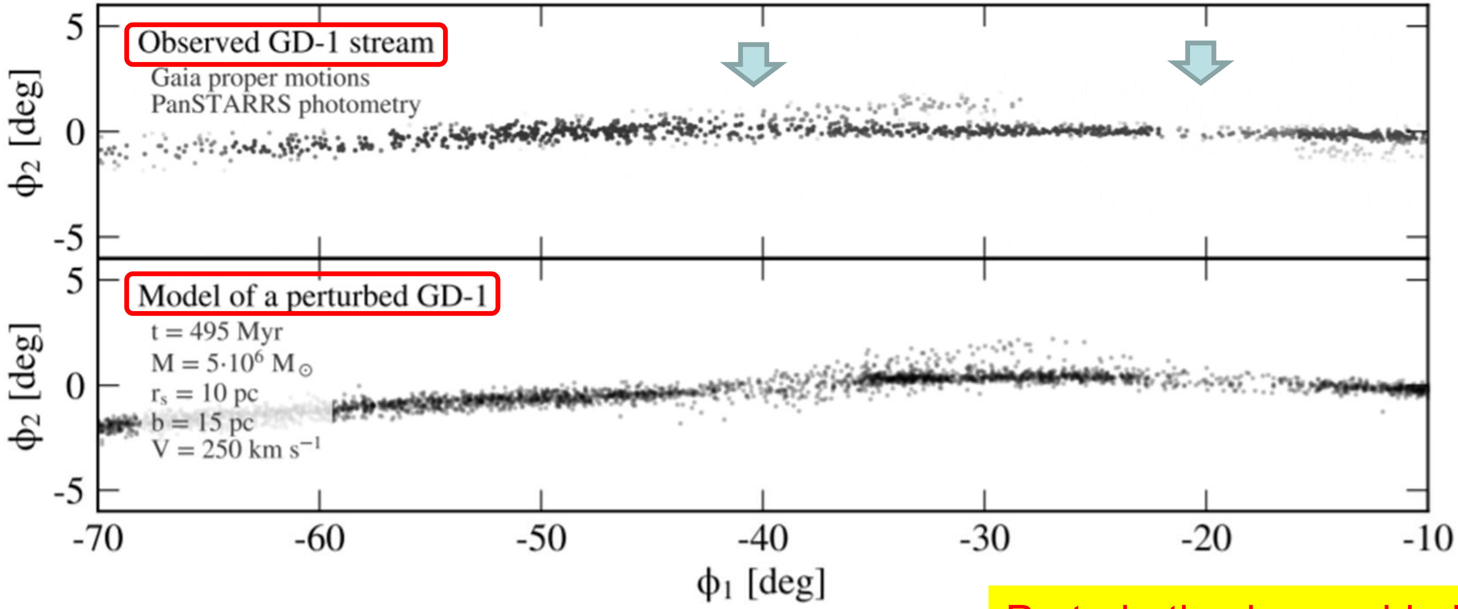

Perturbation by a subhalo?

Figure 1. (Top) Likely members of the GD-1 stellar stream, cleanly selected using Gaia proper motions and PanSTARRS photometry, reveal two significant gaps located at $\phi_1 \approx -20^\circ$ and $\phi_1 \approx -40^\circ$, and dubbed G-20 and G-40, respectively. There is a long, thin spur extending for $\approx 10^\circ$ from the G-40 gap. (Bottom) An idealized model of GD-1, whose progenitor disrupted at $\phi_1 \approx -20^\circ$ to produce the G-20 gap, and which has been perturbed by a compact, massive object to produce the G-40 gap. The orbital structure of stars closest to the passing perturber is distorted into a loop of stars that after 0.5 Gyr appears as an underdensity coinciding with the observed gap, and extends out of the stream similar to the observed spur.

Limits on the abundance of DM subhalos from GD-1 and Pal 5 streams

Banik+2019
arXiv:1911.02663
Banik+2021
MN, 502, 2364

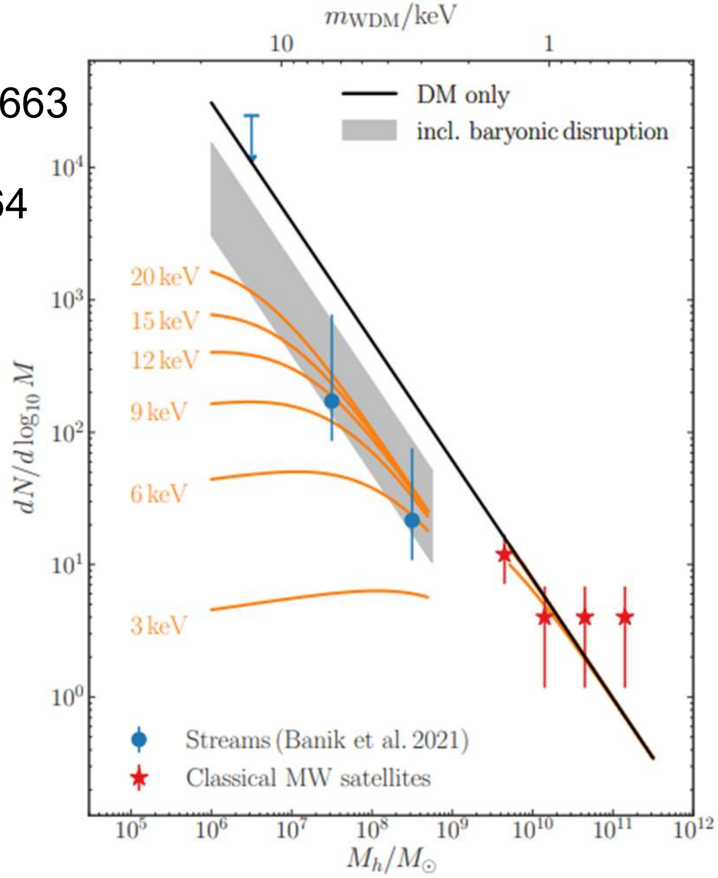

Figure 3. SHMF in the mass range $10^6-10^9 M_\odot$ reconstructed from the analysis of the perturbations induced on the GD-1 and Pal 5 streams. Red data points show the observed classical Milky Way satellites out to 300 kpc. The blue downward arrow and data points show the 68% upper bound, and the measurement and 68% error, respectively, in 3 mass bins below the scale of dwarfs, as obtained in B21 and extrapolated out to 300 kpc to place them on the same SHMF as the red points. The shaded area show the CDM mass function taking into account the baryonic disruption of the subhalos. The orange lines show the predicted mass function for thermal WDM candidates of different mass, taking into account the expected subhalo depletion due to baryonic disruption for the low-mass ($M < 10^9 M_\odot$) measurements from the inner Milky Way.

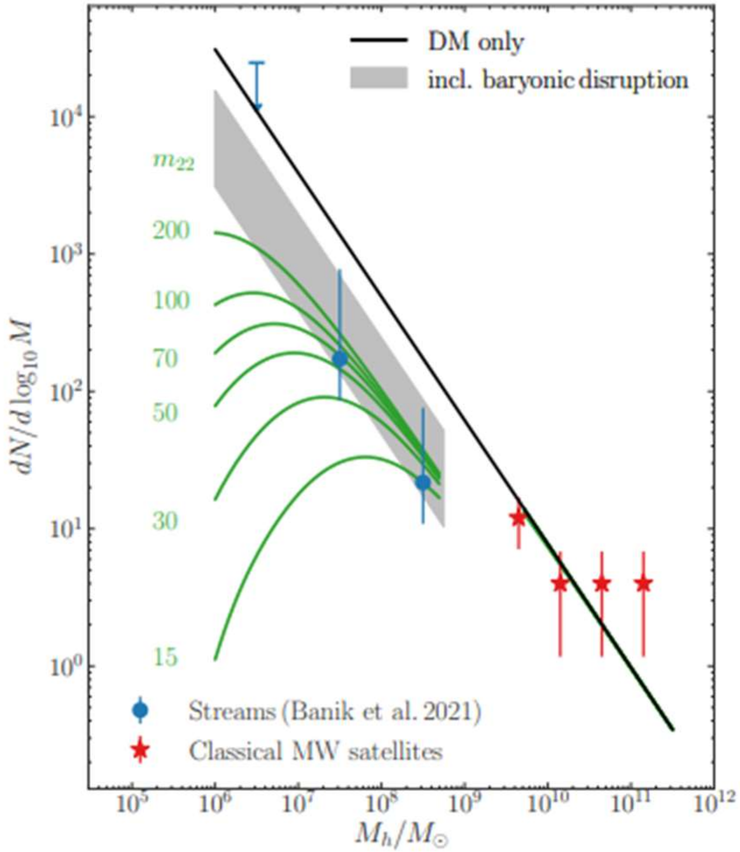

Figure 6. Milky Way SHMF compared with fuzzy DM models for different FDM masses. Data, black line, and gray band are as in Fig. 3, but green curves now show predicted SHMFs for fuzzy DM models with different FDM masses $m_{22} = m_{\rm FDM}/10^{-22}$ eV.

Lens mapping of CDM subhalos

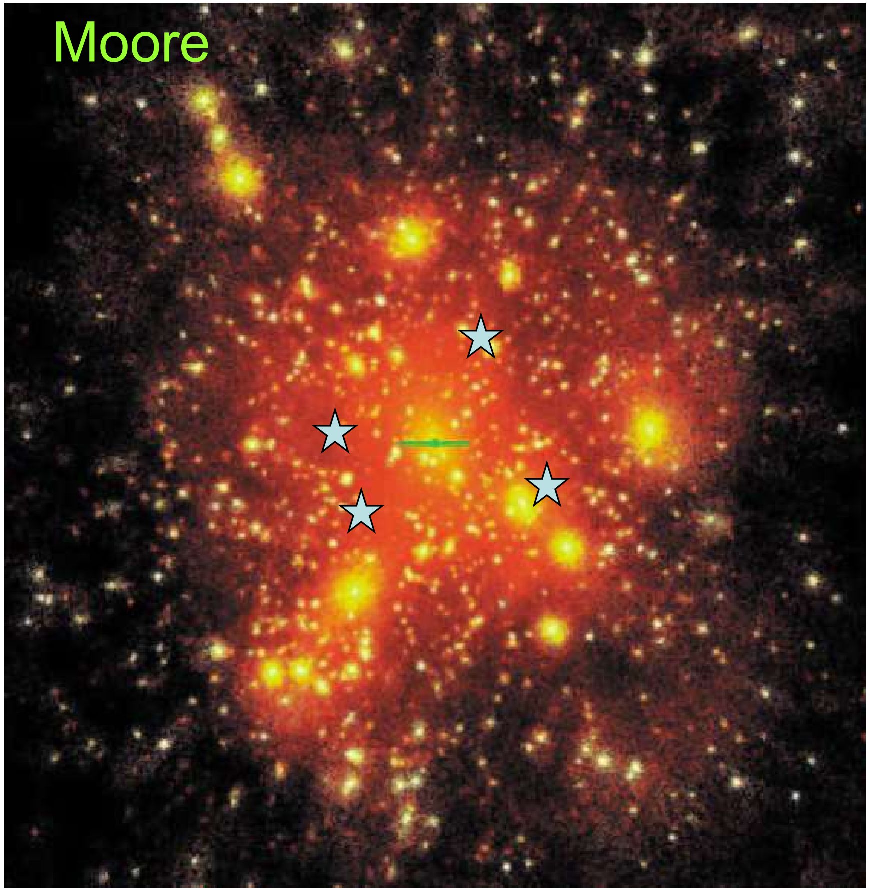

"Anomalous Flux Ratios" for multiply lensed QSOs
(Metcalf & Madau 2001, Chiba 2002, Dalal & Kochanek 2002)

These are hardly explained by smooth lens models.

PG1115+080
(radio quiet)
z_S=1.72, z_L=0.31

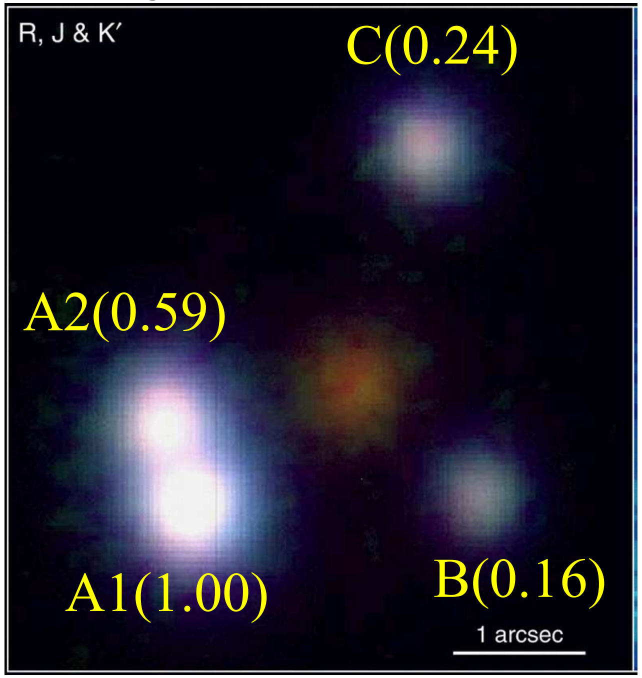

Iwamuro et al. 2000

Smooth lens model
(Singular Isothermal Ellipsoid
+ External Shear)
(Chiba 2002)

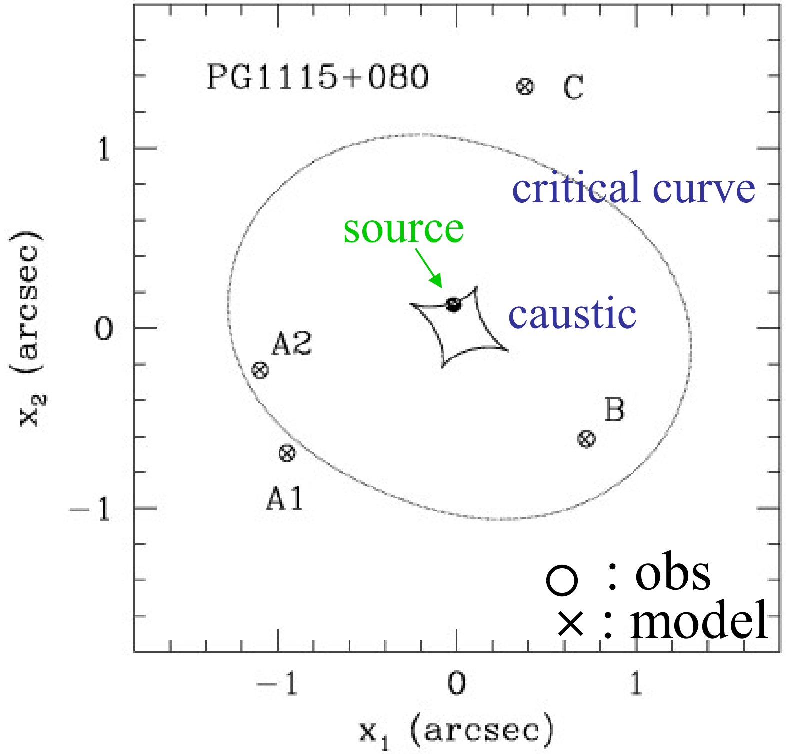

Model: A2/A1 ≈ 1 (fold caustic)

Observed A2/A1 (near-IR): ≈ 0.59 – 0.67 (anomalous)

B1422+231
(radio loud)
z_S=3.62, z_L=0.34

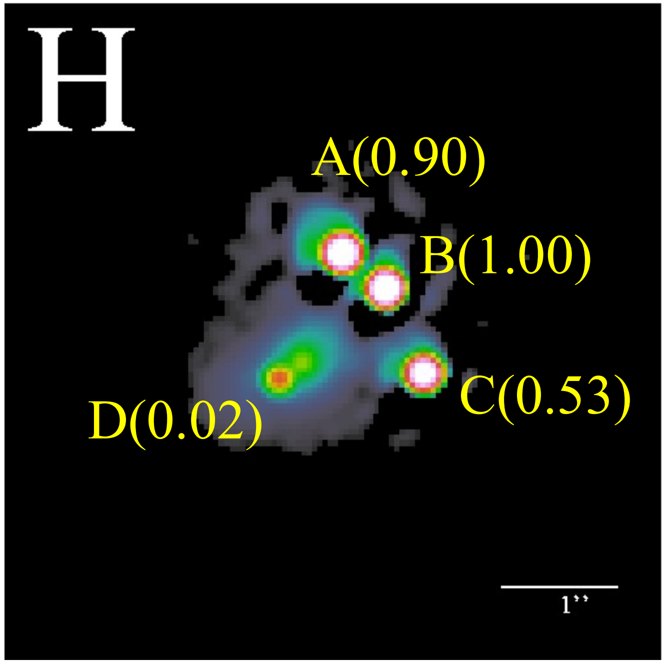

CASTLES

Smooth lens model
(Singular Isothermal Ellipsoid
+ External Shear)

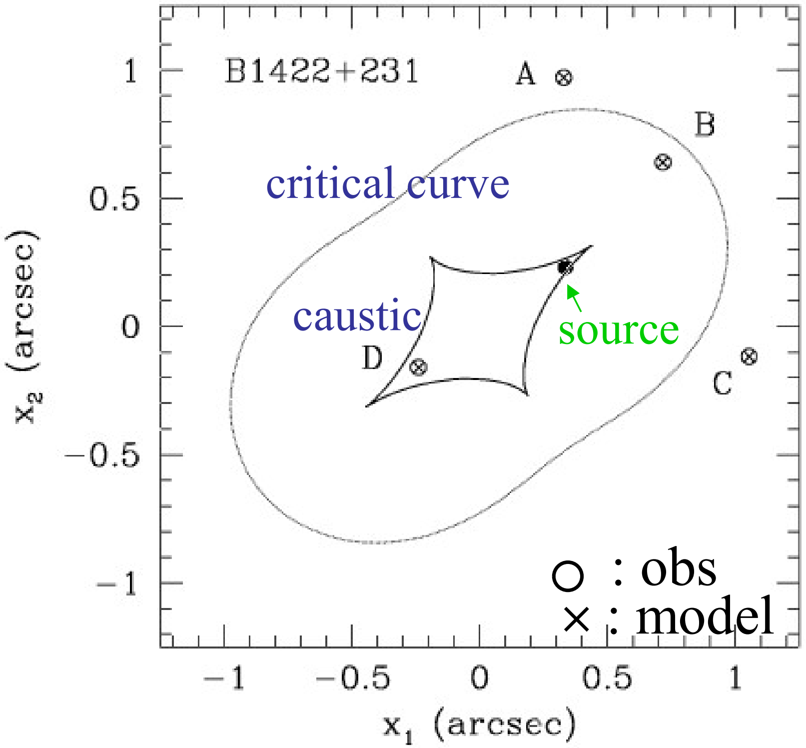

Model: (A+C)/B ≈ 1 (cusp caustic)
Observed (A+C)/B (radio): ≈ 1.42 – 1.50 (anomalous)

Elliptical Lens

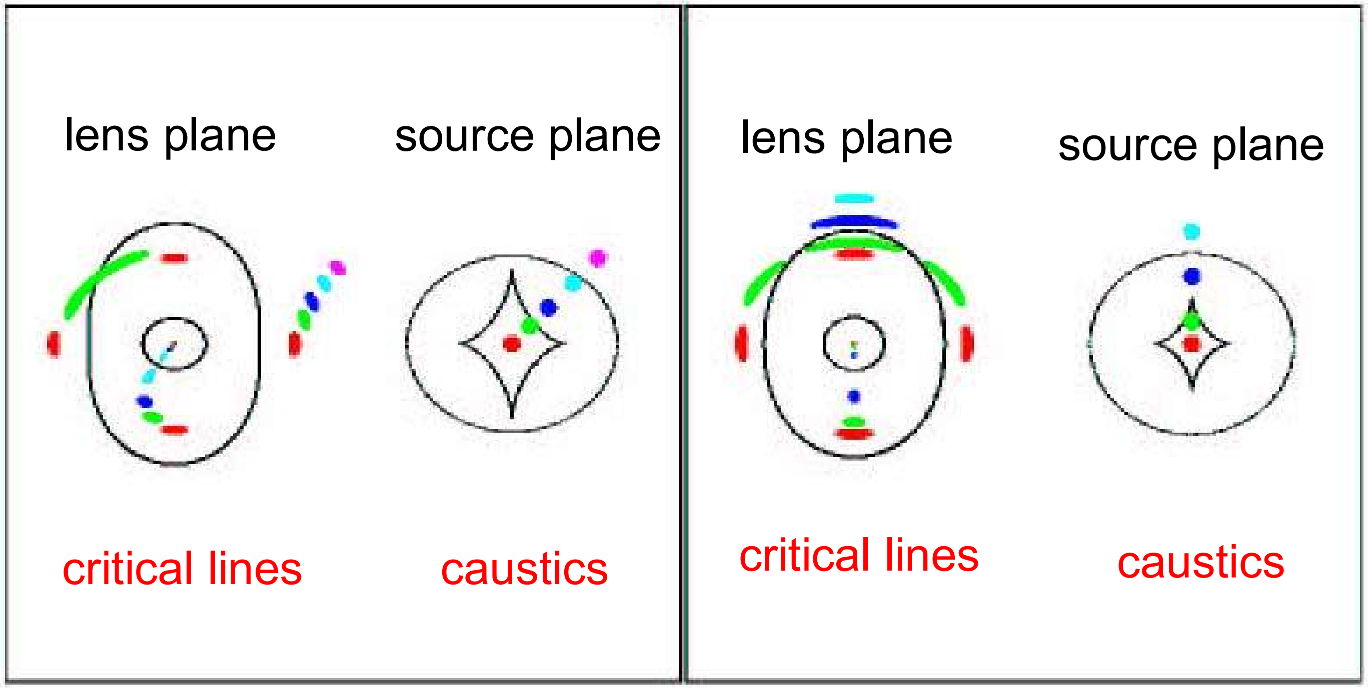

- Fold singularity
- Cusp singularity

Anomalous Flux Ratios

- Implausible by luminous GCs and satellites, CDM subhalos are most likely (Chiba 2002)
- Mass fraction of CDM subhalos ~ a few %
  (Dalal & Kochanek 2002)
- Flux anomaly depends on image parities,
  being consistent with substructure lensing
  (Kochanek & Dalal 2004)

⇒ Evidence for many CDM subhalos!?

Limits on the abundance of WDM subhalos from lensing

Schutz 2021 (arXiv: 2001.05503)

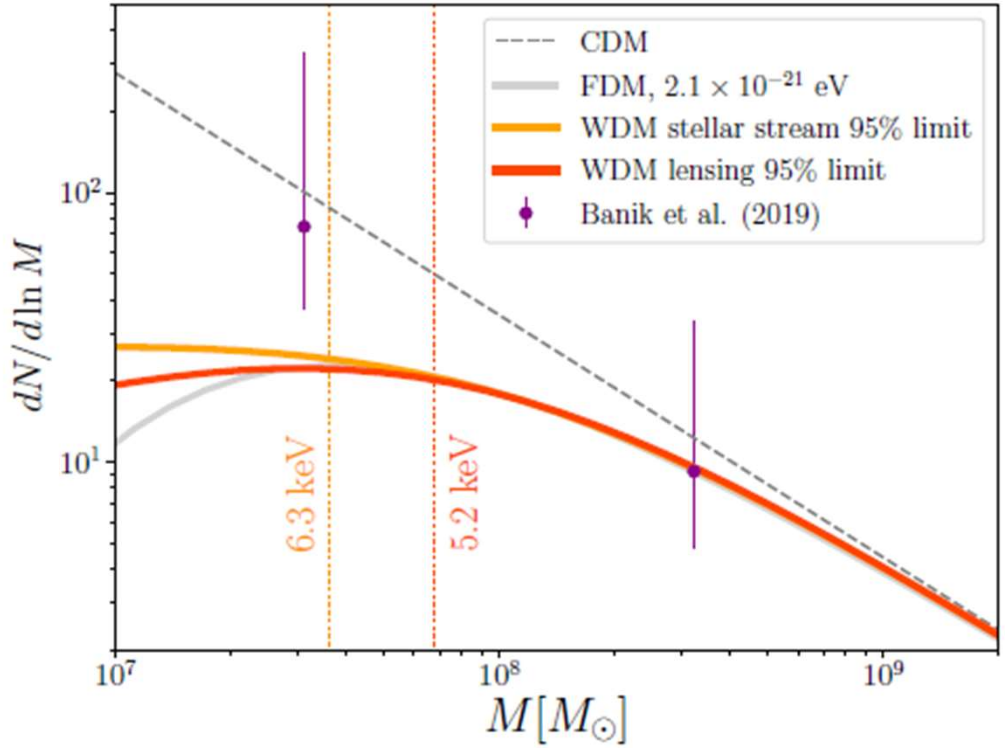

FIG. 1. The SHMF for our mass limit on FDM as compared with the SHMFs for WDM that are constrained by Ref. [7] from stellar streams and Ref. [6] from lensing. Vertical dotted lines show the half-mode mass $M_{\rm hm}$ for the values of m_χ that are excluded in those works. The value of m_{22} shown was chosen to be the maximum value of m_{22} where the predicted suppression of the FDM SHMF is more dramatic than for the excluded WDM cases at all subhalo masses. In this sense, the limits on WDM can be conservatively applied to FDM. Note that all SHMFs have been normalized to match Fig. 3 of Ref. [7] for subhalo masses below $\sim 10^9 M_\odot$, purely for the purposes of comparison of the SHMF shapes. Also note that Refs. [7] and [6] model the WDM SHMF slightly differently as a function of subhalo mass, which gives slightly different SHMF shapes for fixed m_χ.

Summary

- The Milky Way is dominated by a dark halo
  - Halo tracers suggest M_{tot} (MW) = 1 ~ 2 x 10^{12} M_{sun}
  - Sgr stream suggests a nearly spherical shape at 15 < r < 60 kpc, not clear beyond
  - Flat rotation curve suggests $\rho_{tot}(r) \propto r^{-2}$ in the inner part (where a disk dominates), not clear beyond
- Satellite galaxies and small-scale issues
  - Largely dark-matter dominated: (M/L) = 10 ~ 1000
  - Contradiction to CDM predictions:
    - Cored in some galaxies (Core/cusp problem)
    - Mean density is small (Too big to fail problem)
    - Total number is small (Missing satellites problem)

Supplementary slides

Unsolved issues

- Other causes for anomalous flux ratios
  - ✓ Differential dust extinction?
  - ✓ Stellar microlensing?
- Limits on the mass of lens substructure
  - ✓ Mass of a subhalo?
  - ✓ How many subhalos?

Magnification of a source with radius R_s compared with Einstein radius $R_E (\propto M^{1/2})$

Panoramic views of a QSO center

1. Mid-IR imaging of a dust torus

(Near-IR at rest)

- Extinction free
- Microlensing free
- Radio quiet QSOs are available
- Source size is available
  - Hot dust torus at sublimation T of ~1800K
  - Size (inner radius) R_s (~1pc) $\propto L^{1/2}$ from dust reverberation mapping
  - Einstein radius R_E ($\propto M^{1/2}$) vs R_s ⇒ <u>limits on M</u>

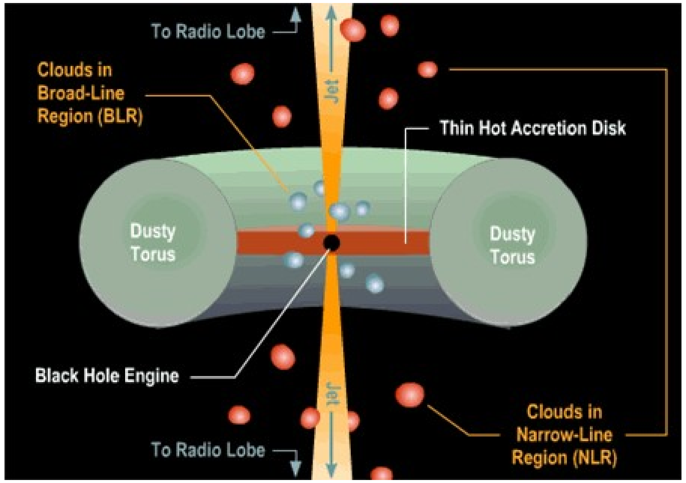

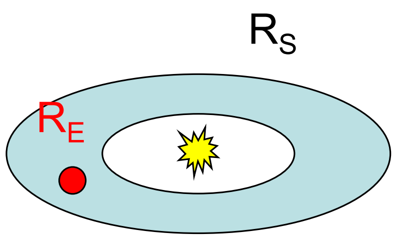

Panoramic views of a QSO center

2. Spectroscopy of NLR and BLR

- NLR: microlensing free
- BLR: affected by microlensing

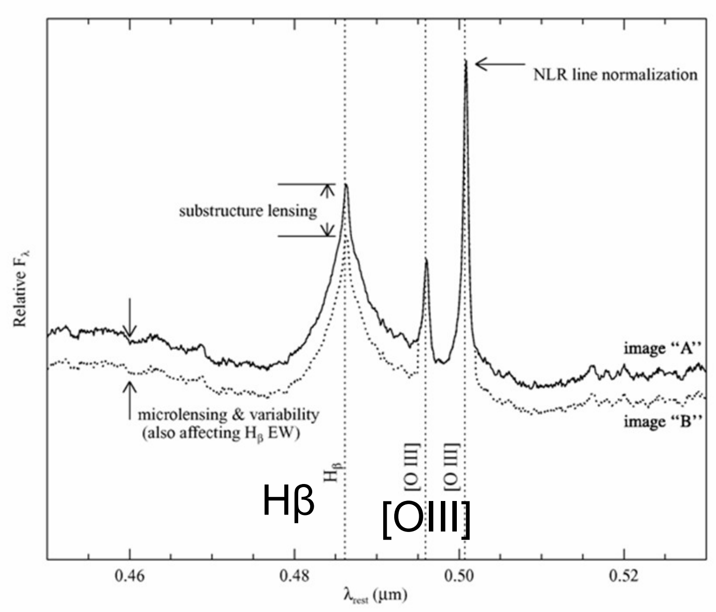

Moustakas & Metcalf 2003

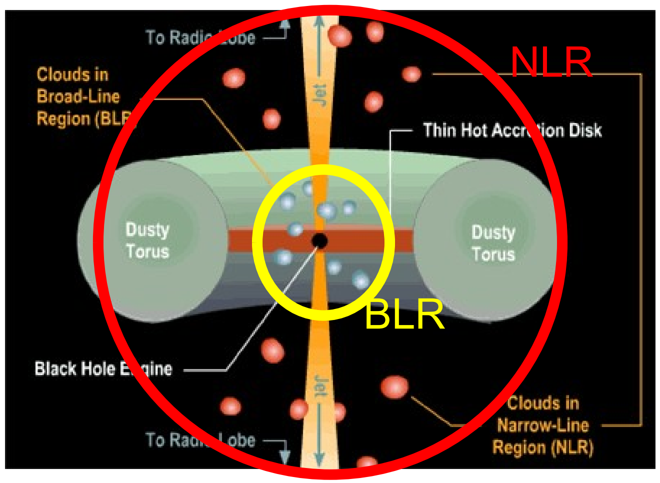

Selective magnification depending on R_E vs R_s
⇒ <u>limits on M</u>

Subaru observations of quadruple lenses

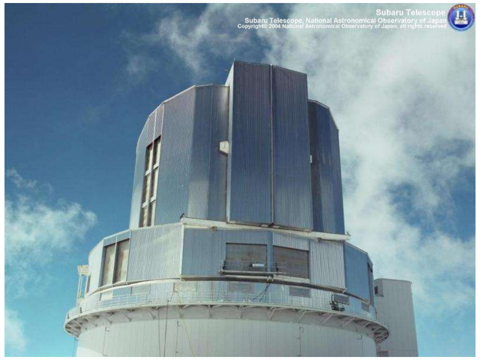

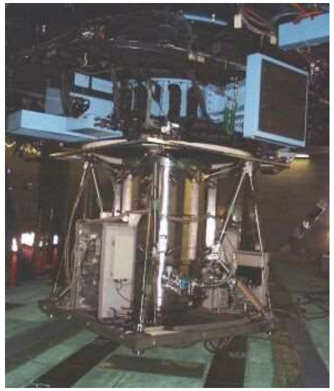

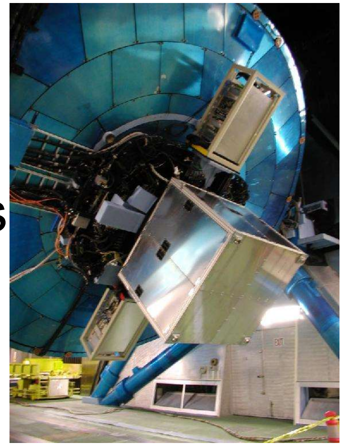

- Mid-IR imaging with COMICS
  (Chiba et al. 2005; Minezaki et al. 2009)
  - FOV=38”×30”, 0.”129/pix
  - N band, λ=11.7μm,
    continuum emission from dust torus
- IFS observation with Kyoto 3DII
  (Sugai et al. 2007)
  - FOV=3”×3”,0.”096 lenslet^{-1},37×37lenslets
  - 0.730 <λ< 0.915μm,
    line emission from NLR and BLR

Subaru image @ 11.7μm

Chiba et al. 2005

PG1115+080

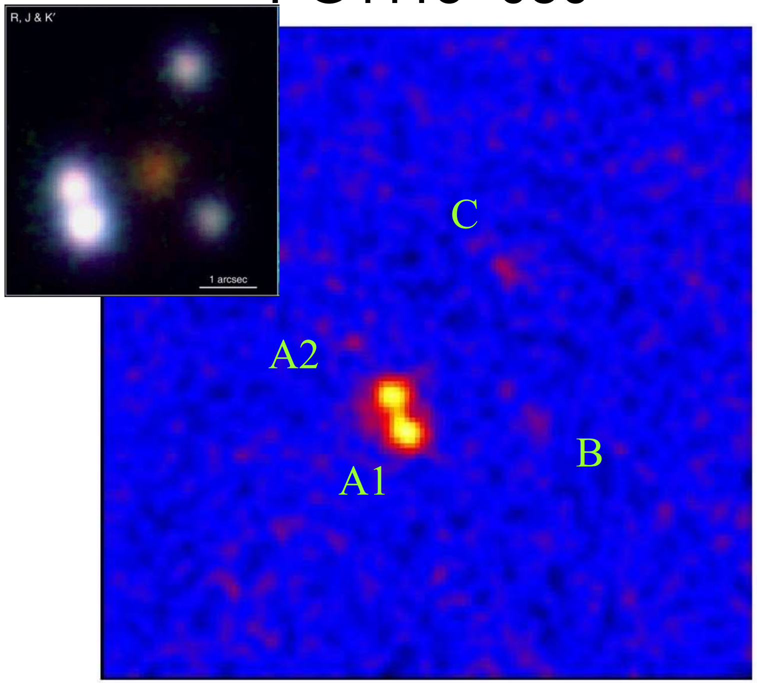

Total flux = 17.5 mJy

A2/A1 (Mid-IR) = 0.93±0.06

(model) ≈ 0.92 fold caustic

(near-IR) = 0.59 ~ 0.67

B1422+231

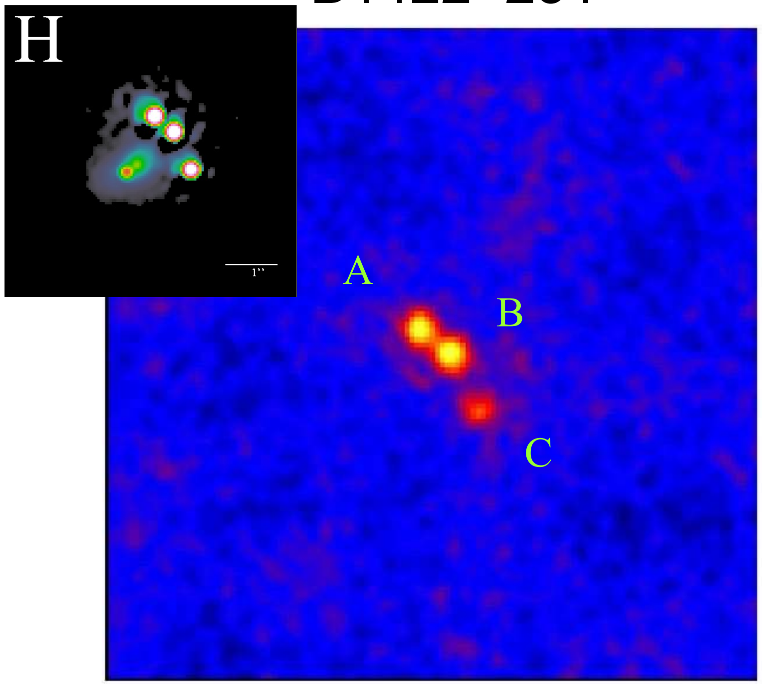

Total flux = 19.2 mJy

(A+C)/B (Mid-IR) = 1.51±0.06

(model) ≈ 1.25 cusp caustic

(radio) = 1.42 ~ 1.50

Subaru image @ 11.7μm

Minezaki et al. 2007

MG0414+0534

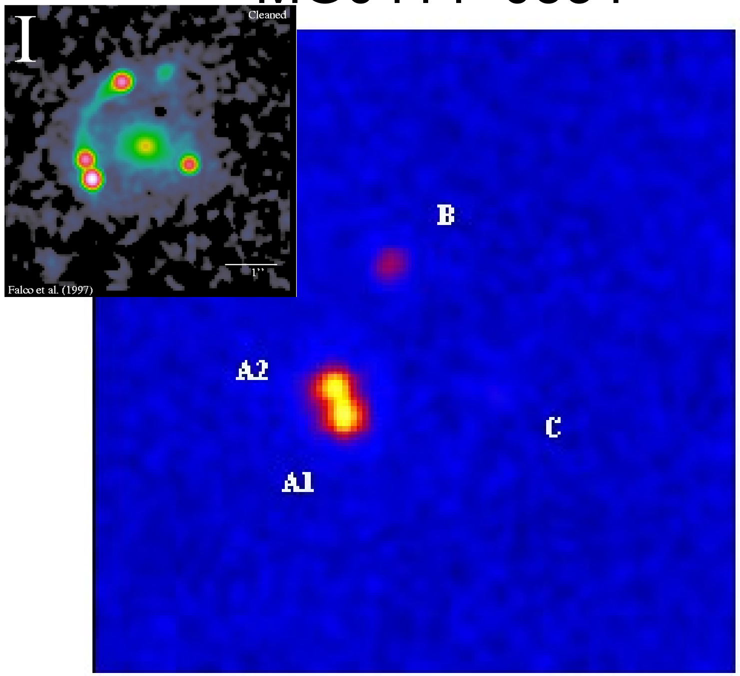

Total flux = 39.2 mJy

A2/A1 (Mid-IR) = 0.90±0.04

(model) ≈ 1.1 fold caustic

(near-IR) = 0.4 ~ 0.8

Q2237+030

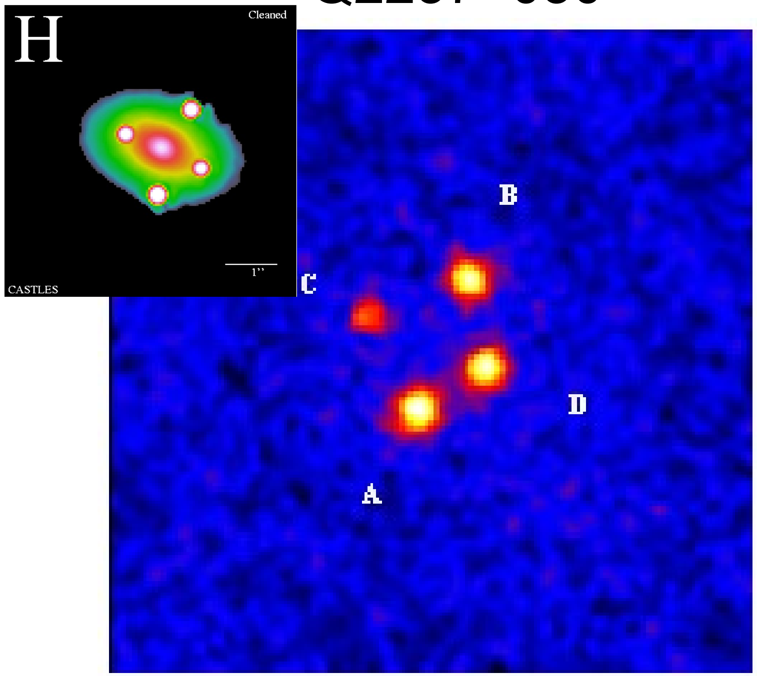

Total flux = 22.2 mJy

B/A (Mid-IR) = 0.84±0.05,

C/A=0.46±0.02, D/A=0.87±0.05

B/A (model) = 0.87,

C/A=0.46, D/A=0.86

IFS data of RXJ1131-1231

Sugai et al. 2007

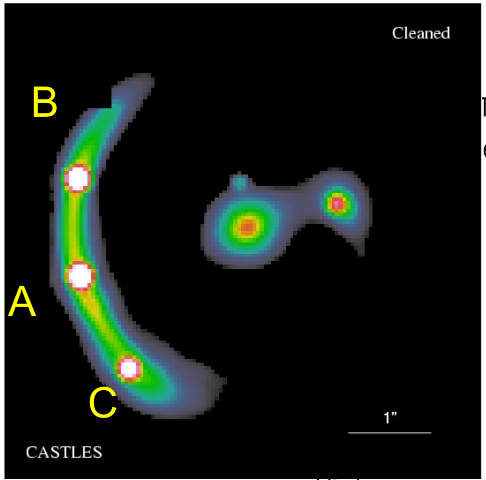

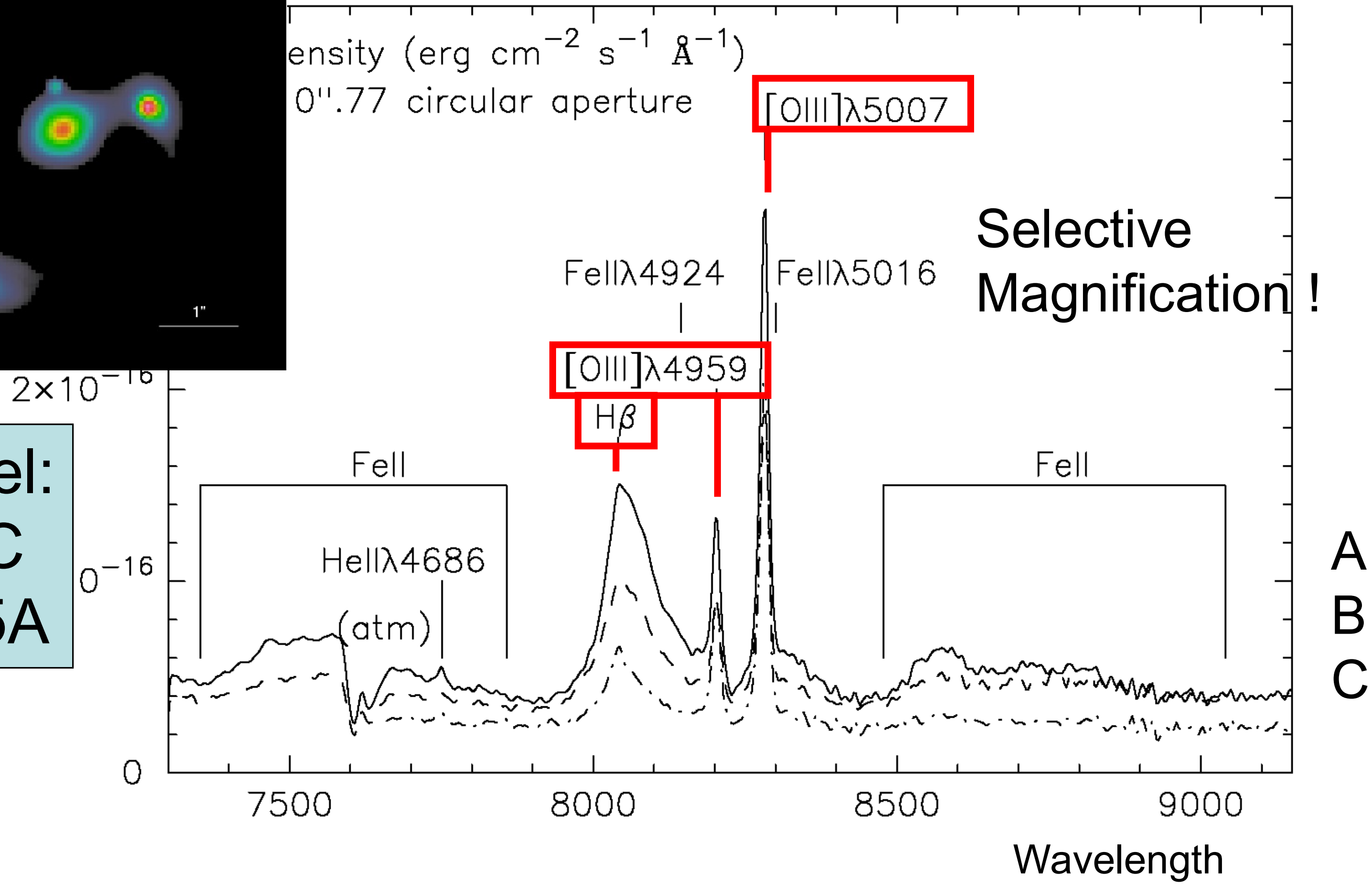

Selective Magnification !

Model:
B ~ C
~ 0.5A

Hβline flux

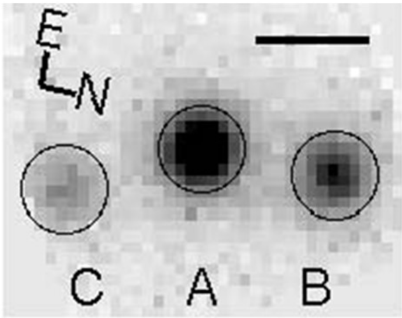

A/B=1.74
C/B=0.46

[O III] line flux

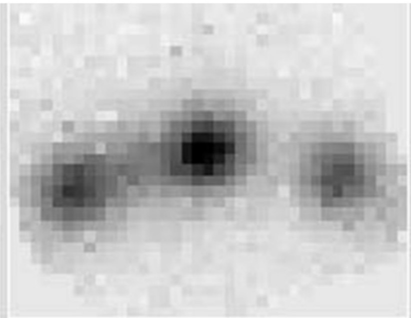

A/B=1.63
C/B=1.19

Smooth model

A/B ≈ 1.7

C/B ≈ 1.0

- NLR([OIII]) is OK
- BLR (Hβ) of Image C is microlensed

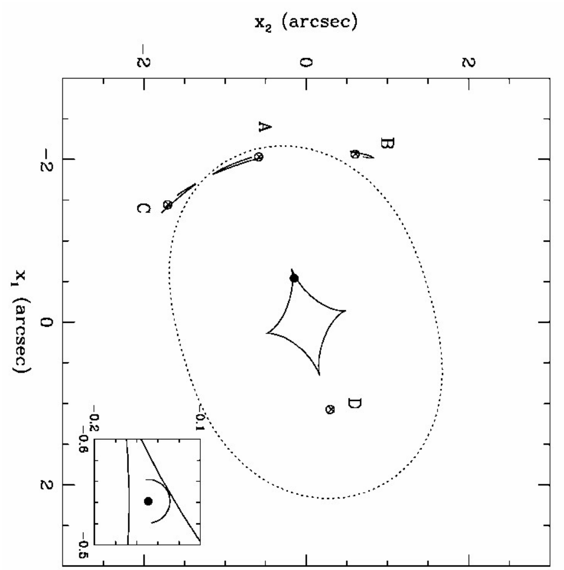

[O III] line flux
(point source subtracted)

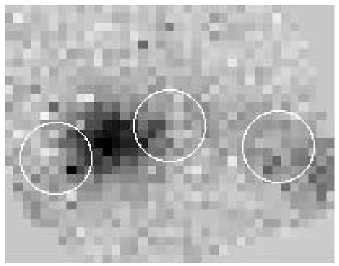

R_s (NLR) ≈ 90pc

Limits on substructure lensing

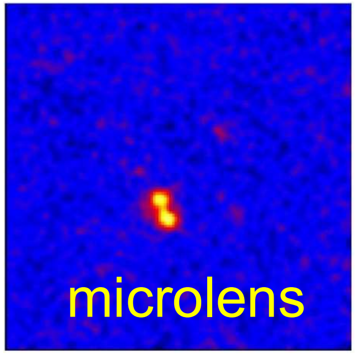

PG1115+080

(A1, A2)

$R_s \sim 1$ pc

Mid-IR flux ratio

$M_E < 16$ Msun

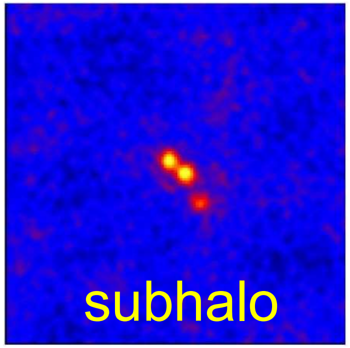

B1422+231

(A, B, C)

$R_s \sim 3$ pc

Mid-IR flux ratio

$M_E > 200$ Msun

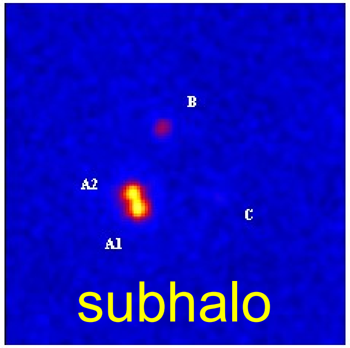

MG0414+0534

(A1, A2)

$R_s \sim 2$ pc

Mid-IR flux ratio

$M_E > 200$ Msun

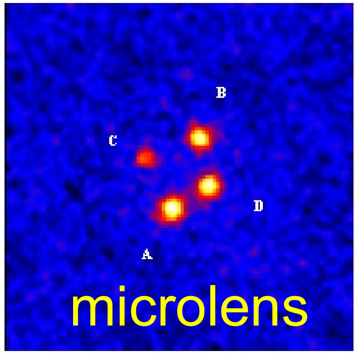

Q2237+030

(A, B, C, D)

$R_s \sim 2$ pc

Mid-IR flux ratio

$M_E < 10$ Msun

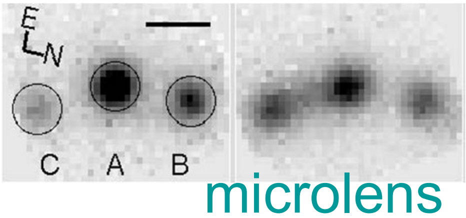

RXJ1131-1231

R_s (BLR) ~ 0.01 pc, R_s (NLR) ~ 100pc

$M_E < 10^5$ Msun for NLR

ALMA observation of gravitationally-lensed, extended images

- Direct imaging of subhalo-lensed images with high resolution observation (10mas)
  - ✓ Determination of subhalo masses
  - ✓ Spatial distribution of subhalos
- Source image：sub-millimeter continuum radiation from dust
  - ✓ T=30~60 K, L=10^2~10^3 pc
  - ✓ S at 850μm=several tens mJy

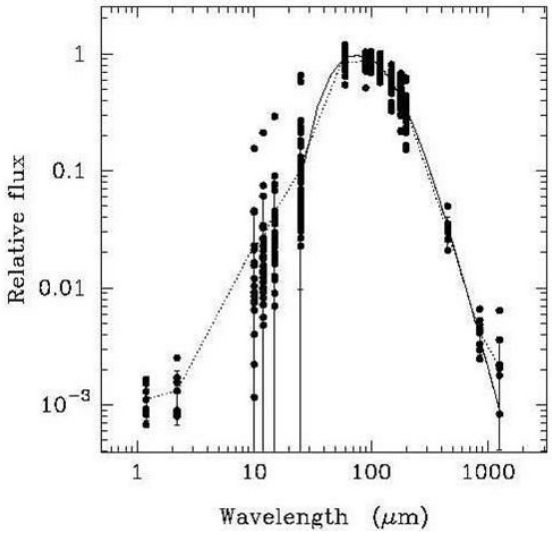

Test for CDM models

ALMA: lensing galaxy SDP.81

Hezaveh et al. 2016

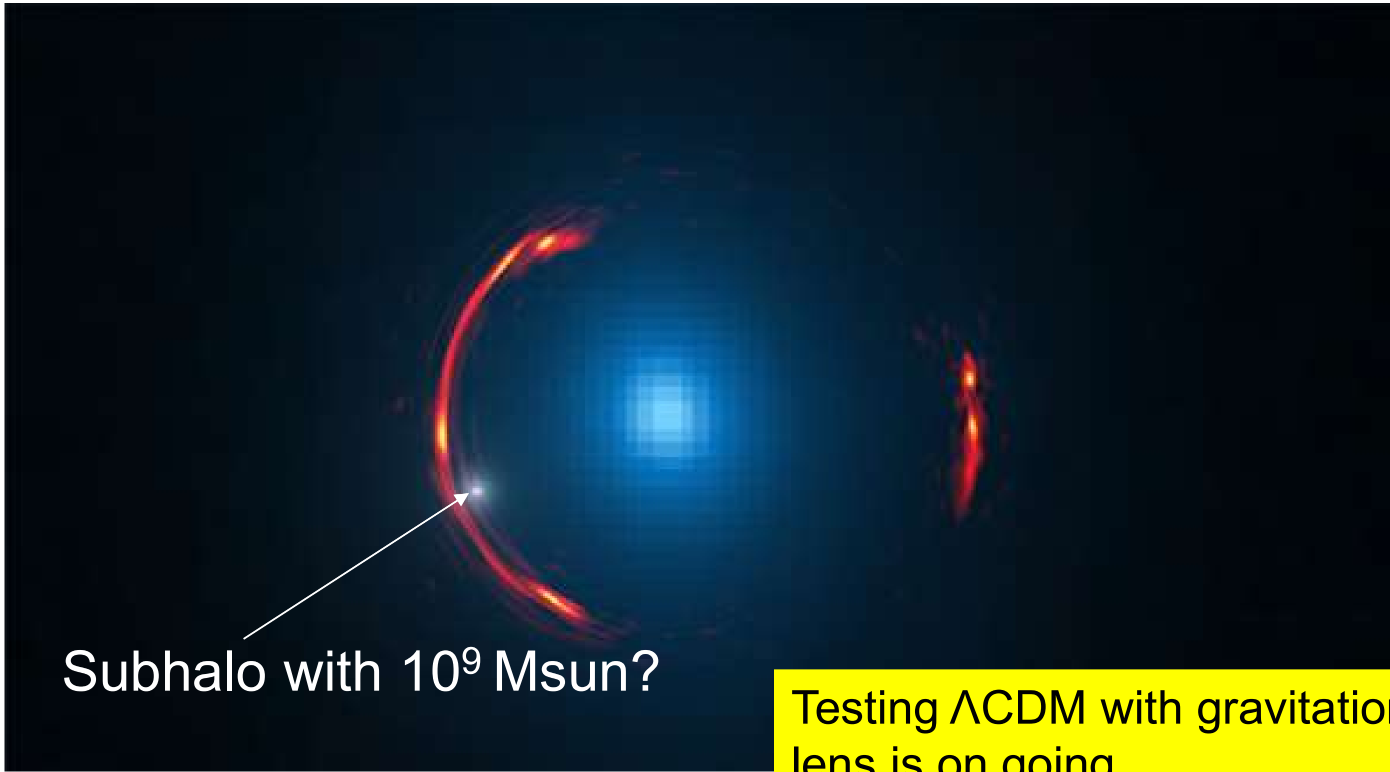

Testing ΛCDM with gravitational lens is on going

Inoue, K. T., Minezaki, Matsushita, Chiba 2016:
showing the effect of under-dense large-scale structures on lensed image
This issue is yet unsettled.